Preprint typeset in JHEP style - HYPER VERSION

hep-th/0311237
ITFA-2003-52
UPR-1055-T
WIS/30/03-NOV-DPP

A Multi-boundary AdS Orbifold and DLCQ Holography:

A Universal Holographic Description of Extremal Black Hole Horizons

Vijay Balasubramanian[1], **Asad Naqvi**[1,2] **and Joan Simón**[1,3]

1. *David Rittenhouse Laboratories, The University of Pennsylvania, Philadelphia, PA 19104-6396, U.S.A.*
2. *Instituut voor Theoretische Fysica, Valckenierstraat 65, 1018XE Amsterdam, The Netherlands*
3. *The Weizmann Institute of Science, Herzl Street 2, 76100 Rehovot, Israel*

vijay@endive.hep.upenn.edu, anaqvi@science.uva.nl, jsimon@bokchoy.hep.upenn.edu

Abstract: We examine a stationary but non-static asymptotically AdS_3 spacetime with two causally connected conformal boundaries, each of which is a "null cylinder", namely a cylinder with a null direction identified. This spacetime arises from three different perspectives: (i) as a non-singular, causally regular orbifold of global AdS_3 by boosts, (ii) as a Penrose-like limit focusing on the horizon of extremal BTZ black holes, and (iii) as an S^1 fibration over AdS_2. Each of these perspectives sheds an interesting light on holography. Examination of the conformal boundary of the spacetime shows that the dual to the space should involve DLCQ limits of the D1-D5 conformal field theory. The Penrose-like limit approach leads to a similar conclusion, by isolating a sector of the complete D1-D5 CFT that describes the physics in the vicinity of the horizon of an extremal black hole. As such this is a holographic description of the universal horizon dynamics of the extremal black holes in AdS_3 and also of the four and five dimensional stringy black holes whose states were counted in string theory. The AdS_2 perspective draws a connection to a $0+1$d quantum mechanical theory. Various dualities lead to a Matrix model description of the spacetime. Many interesting issues that are related to both de Sitter physics and attempts to "see behind a horizon" using AdS/CFT arise from (a) the presence of two disconnected components to the boundary, and (b) the analytic structure of bulk physics in the complex coordinate plane.

Keywords: AdS orbifolds, holography, time dependence, matrix models, BTZ, Penrose-like limits.

Contents

1. Introduction

There are several issues concerning string theory in time dependent spacetimes that we would like to study using holography. First, we would like to gain insight into the resolution of singularities localized in time such as those that occur inside black holes and at the big bang. Second, we would like to understand how and whether physics behind a horizon is represented and whether the information loss paradox for black holes is avoided. Third, we would like to understand how holography and quantum gravity work in the presence of a positive cosmological constant. Finally, we would like to have simple solvable examples of time-dependent universes in string theory, that avoid pitfalls such as closed causal curves and large back reaction that make typical constructions such as boost orbifolds difficult to define consistently and to understand.[1] In many of the cases that have been studied, such as the eternal black hole [3, 4, 5, 6] and de Sitter space [7], one of the challenges that arises is that the spacetime has multiple disconnected components to its conformal boundary[2]. If holographic duals are to be associated with the conformal boundary of a space it is necessary to understand how the theories associated each disconnected component are related.

In this paper we study an orbifold of AdS_3 by two boosts which does not have closed causal curves. In terms of AdS_3 as an $SL(2,R)$ group manifold, the orbifold is an identification by a hyperbolic element of the left $SL(2,R)$ action. The orbifold is closely related to the extremal BTZ [9] spacetimes, but is nevertheless not a black hole – there is neither a horizon nor a singularity. However, like an eternal black hole and like de Sitter space, the spacetime has two disconnected components to its conformal boundary. Unlike the former cases the two boundary components are causally connected. At first sight this appears to violate a no go theorem due to Galloway et al. [10] which says that in three dimensions or higher, any Lorentzian AdS spacetimes with multiple boundaries also have horizons. However, as we will see, our 3d orbifold contains a circle of fixed size. Compactifying on this circle gives rise to a 2d AdS geometry with flux which is outside the conditions required for the theorem of [10].

Each of the boundary components is a "null cylinder", namely a cylinder in which a lightlike direction has been identified, or equivalently the infinite momentum boost of the usual cylinder with a spacelike identification. Indeed, the timelike surfaces at fixed radial coordinate are literally conformal to boosted cylinders with the boost approaching infinity as the spacetime boundary is reached. The space, which has appeared before as the "self-dual" AdS_3 geometry of Coussaert and Henneaux [11], can be understood in many ways. It also arises from a Penrose-like limit focusing on the horizon of extremal BTZ black holes [12, 13, 14], as discussed by Strominger and collaborators. Thus it is the universal description of the vicinity of the horizon in all of the extremal finite-area black holes whose entropy has been explained in string theory. Finally, the orbifold can be seen as a circle fibration of AdS_2 or, equivalently, AdS_2 with a constant flux turned on.

To study holography in the orbifold the first step is to extract the normalizable and non-normalizable fluctuations of bulk field theory to assemble a holographic dictionary and prescription

[1] Recent relevant work includes [1, 2].

[2] Interesting prior work exploring the entropy of dS black holes from the perspective of the Chern-Simmons approach to 3d gravity appears in [8].

for computing correlations. By exploring unitary representations of the $SL(2,R) \times U(1)$ isometry group that survives the orbifold projection we find a quantized spectrum of normalizable modes corresponding to states in the dual field theory [15]. Modes with positive (negative) angular momentum are localized closer to the right (left) boundary of the spacetime. From the perspective of directly solving the wave equation on the orbifold the same spectrum is obtained by requiring single valuedness of wavefunctions in the complex coordinate plane. This requirement of an absence of cuts in the complex plane is reminiscent of other recent work in which the structure of amplitudes and wavefunctions in the complex plane was important for the structure of holography in the BTZ black hole background [5, 6].

We also obtain the non-normalizable modes that correspond to sources in the dual field theory [15]. Again requiring the absence of cuts in the complex coordinate plane requires a particular addition of normalizable modes to the non-normalizable basis, thus choosing a distinguished vacuum. The non-normalizable modes diverge on both boundaries simultaneously suggesting that it is not possible to turn on independent sources for components of the dual that are associated with each boundary. However, on closer examination it turns out that in fact the correlation is between sources at real positions on one boundary and shifted in the complex coordinate plane in the other. Boundary data, and thus dual sources, at real positions are in fact independent. Indeed, it turns out that the non-normalizable modes in the BTZ black hole also diverge at both boundaries in a similar way. Since there are two disconnected, but entangled, components to the dual in that case, a similar picture is suggested in our case also. The standard calculation of CFT 2-point correlators from the bulk on-shell action [16] takes contributions from both boundaries. However, by expressing the calculation in terms of data at one or both boundaries we can compute correlation function on each boundary component or between them. We also compute a bulk-boundary propagator on the orbifold by calculating the bulk Feynman propagator from a sum on images and then taking a bulk point to the boundary. From this perspective, the dual two-point function arises from taking both bulk points to a boundary; so it is possible to compute separate correlators in each dual component, as well as between them. The results match the on-shell calculation, and we find that the correlation function between boundaries is obtained from the one within a boundary by certain shifts of the arguments in the complex coordinate plane. This situation, involving analytic relations between different correlators via excursions in the complex coordinate plane is strongly reminiscent of the holography in the BTZ black hole [5, 6].

The various perspectives from which our spacetime arises (as an orbifold of AdS_3, as a space with two null cylinder boundaries, as an AdS_2 fibration, and as a Penrose-like limit of the D1-D5 system) give us a number of tools for studying the dual field theory. Recall first that the dual to global AdS_3 spacetime is the D1-D5 CFT, namely a sigma model on the target space $K3^N/S_N$ (or $T4^N/S_N$ depending on how AdS_3 is embedded in string theory). Then, as an orbifold of AdS_3, the dual theory should be an orbifold of the D1-D5 CFT by a certain left-moving conformal transformation. States that survive the orbifold are characterized by their right-moving $SL(2,R)$ representation and an integer $U(1)$ charge from the left-moving side. Of course these surviving symmetries match the isometries of the bulk orbifold. As a space with two null cylinder boundaries

in causal contact, our orbifold should be dual to two CFTs each of which is Discrete Light Cone Quantized (DLCQ). Finite energy states in a DLCQ CFT carry momenta in only the left-moving (or right-moving) direction. The two boundaries in our orbifold each produce a tower of positive (negative) integer momenta which together match the complete tower of states in the conformal-orbifold picture. There is also a nice correspondence with the fact that normalizable modes in the bulk are localized closer to one boundary or the other depending on the direction in which they rotate, or equivalently the sign of their $U(1)$ charge. The origin of our spacetime in a Penrose-like limit focusing on the horizons of extremal BTZ black holes allows us to isolate a sector of the D1-D5 CFT that describes this region – an entangled state of the DLCQ of the D1-D5 string makes an appearance. The perspective that the spacetime is an AdS_2 fibration suggests that our orbifold should be related to a $0+1$d quantum mechanics. Finally, various S and T dualities, combined with lifts to M-theory lead to Matrix model descriptions of our spacetime.

2. Classical geometry

Three dimensional anti-de Sitter space (AdS_3) is a maximally symmetric space of constant negative curvature. It is the hyperboloid

$$\begin{aligned} \mathrm{AdS}_3 &\hookrightarrow \mathbb{R}^{2,2} \\ -u^2 - v^2 + x^2 + y^2 &= -l^2 \quad , \end{aligned} \tag{2.1}$$

in flat $\mathbb{R}^{2,2}$. By construction, the isometry group is $\mathrm{SO}(2,2)$ [3].

A global parametrization of AdS_3 is obtained by solving (2.1) in terms of

$$\begin{aligned} u = l\,\cosh\rho\,\cos\tau \quad &, \quad v = l\,\cosh\rho\,\sin\tau \\ x = l\,\sinh\rho\,\cos\theta \quad &, \quad y = l\,\sinh\rho\,\sin\theta\ . \end{aligned} \tag{2.2}$$

The induced metric is

$$g_{AdS_3} = l^2\left[-(\cosh\rho)^2(d\tau)^2 + (d\rho)^2 + (\sinh\rho)^2(d\theta)^2\right]. \tag{2.3}$$

As usual, we shall refer to AdS_3 as the universal covering space of the above hyperboloid (2.1) in which the global timelike coordinate τ has been unwrapped (i.e. take $-\infty < \tau < \infty$). The Killing vectors of the metric generate the Lie algebra $\mathfrak{so}(2,2)$ of the isometry group, and are described in terms of the embedding space $\mathbb{R}^{2,2}$ as

$$J_{ab} = x_b\partial_a - x_a\partial_b\ , \tag{2.4}$$

with $x^a \equiv (u,v,x,y)$ and $x_a = \eta_{ab}\,x^b$, with $\eta_{ab} = (-,-,+,+)$. We can decompose $\mathfrak{so}(2,2) = \mathfrak{sl}(2,\mathbb{R}) \oplus \mathfrak{sl}(2,\mathbb{R})$ via the linear combinations

$$\xi_1^{\pm} = \frac{1}{2}(J_{01} \pm J_{23}) \ \ ; \ \ \xi_2^{\pm} = \frac{1}{2}(J_{02} \pm J_{13}) \ \ ; \ \ \xi_3^{\pm} = \frac{1}{2}(J_{03} \mp J_{12})\,, \tag{2.5}$$

[3] The isometry group of the geometry is really $\mathrm{O}(2,2)$ but when embedded in string theory, the presence of fluxes restricts this to $\mathrm{SO}(2,2)$.

where $\xi_i^{\pm}$ satisfy the non-vanishing commutation relations

$$[\xi_i^{\pm}, \xi_j^{\pm}] = \epsilon_{ijk}\, \xi_k^{\pm}\,. \tag{2.6}$$

Discrete quotients of AdS_3 involving a single generator are classified by the set of inequivalent uniparametric subgroups of $\mathrm{SO}(2,2)$ [9, 17, 18]. We will consider quotients by the action of a subgroup of $\mathrm{SO}(2,2)$ isomorphic to $\mathbb{Z}$.

$$\mathrm{P} \to e^{t\xi}\mathrm{P} \quad , \quad t = 0, \pm 2\pi, \pm 4\pi, \cdots \quad \forall\, \mathrm{P} \in \mathrm{AdS}_3,$$

where

$$\xi = \frac{1}{2}\left(J_{02} + J_{13}\right)\ . \tag{2.7}$$

This generator is a linear combination of a boost in the ux-plane and vy-plane in the embedding space $\mathbb{R}^{2,2}$.

It is instructive to compare the space obtained after this identification with the BTZ black hole. The latter is obtained by identifying AdS_3 by the discrete action generated by the Killing vector [9]

$$\xi_{\mathrm{BTZ}} = \frac{r_+}{l} J_{12} - \frac{r_-}{l} J_{03} - J_{13} + J_{23}. \tag{2.8}$$

In the non-extremal case, $r_+^2 - r_-^2 > 0$ and by a $\mathrm{SO}(2,2)$ transformation, ξ_{BTZ} can be brought into the form:

$$\xi'_{\mathrm{BTZ}} = \frac{r_+}{l} J_{12} - \frac{r_-}{l} J_{03}. \tag{2.9}$$

The mass and angular momentum of the black hole are given by

$$M = \frac{1}{l^2}(r_+^2 + r_-^2) \quad , \quad J = \frac{2}{l} r_+ r_-. \tag{2.10}$$

The extremal black hole is obtained by taking the limit $r_+ \to r_-$ in (2.8), so that the generator becomes

$$\xi_{BTZ} \to \frac{r_+}{l}\left(J_{12} - J_{03}\right) - J_{13} + J_{23}\ . \tag{2.11}$$

After a rotation in the $\{x^2, x^3\}$ plane by $\pi/2$ this vector field becomes

$$\xi_{BTZ} \to \frac{r_+}{l} 2\xi + J_{12} + J_{23}\ . \tag{2.12}$$

where ξ is the generator (2.7) of our orbifold spacetime. Thus the extremal BTZ identification differs from the one generating our spacetime by the extra action generated by $J_{12} + J_{23}$. The alert reader might worry that the generator ξ'_{BTZ} which is a $SO(2,2)$ rotation of ξ_{BTZ} does appear to approach our orbifold generator after a further rotation in the $\{x^2, x^3\}$ plane when we take the extremal limit $r_- \to r_+$. However, this is misleading – the $SO(2,2)$ transformation relating (2.8) to (2.9) does not exist in the $r_- \to r_+$ limit. Indeed, the generator of the extremal BTZ black hole lies in a different orbit of $SO(2,2)$ than the generator of the self-dual orbifold.

2.1 Bulk geometry

By construction, any discrete quotient of AdS_3 is locally isometric to AdS_3, but differs from it globally. A unique feature of (2.7) is that it is the only generator giving rise to a smooth discrete quotient of AdS_3 preserving one half of the supersymmetries. This feature is inherited by any higher dimensional AdS spaces. Here, by smoothness, we mean absence of fixed points and closed causal curves. That there are no fixed points can be seen from the point of view of the embedding space $\mathbb{R}^{2,2}$, where the only fixed point is the origin ($u = v = x = y = 0$), since Lorentz transformations act linearly in $\mathbb{R}^{2,2}$. However, the origin does not belong to AdS_3; hence the absence of fixed points.

To show the absence of closed causal curves, and also to gain some insight concerning the geometry of the identifications, it is convenient to parametrize AdS_3 in the adapted coordinates [11]:

$$\begin{aligned} u &= l\left(\cosh z\cosh\phi\cos t + \sinh z\sinh\phi\sin t\right), \\ v &= l\left(\cosh z\cosh\phi\sin t - \sinh z\sinh\phi\cos t\right), \\ x &= l\left(\cosh z\sinh\phi\cos t + \sinh z\cosh\phi\sin t\right), \\ y &= l\left(\cosh z\sinh\phi\sin t - \sinh z\cosh\phi\cos t\right). \end{aligned} \tag{2.13}$$

In these coordinates, the AdS_3 metric is

$$g = l^2\left(-(dt)^2 + (d\phi)^2 + 2\sinh(2z)dtd\phi + (dz)^2\right), \tag{2.14}$$

and, before making any identification, all coordinates are taken to be non-compact, $-\infty < t\,,\phi\,,z < \infty$.

Since the action of the generator (2.7) in the adapted coordinate system (2.13) is given by a simple shift along the ϕ direction,

$$2\xi = \frac{\partial}{\partial\,\phi}\,,$$

the description of the discrete quotient is given by making ϕ an angular coordinate taking values in $[0\,,2\pi)$. Notice that the effective radius of the circle is constant and equal to the radius of AdS_3, l.

It is now easy to prove the non-existence of closed causal curves [11]. We begin by assuming that such a closed causal curve exists. Then, if $x^\mu(\lambda)$ is the embedding of this curve with λ being its affine parameter, the norm of its tangent vector satisfies the condition

$$-\left(\frac{dt}{d\lambda}\right)^2 + \left(\frac{dz}{d\lambda}\right)^2 + \left(\frac{d\phi}{d\lambda}\right)^2 + 2\sinh 2z\frac{dt}{d\lambda}\frac{d\phi}{d\lambda} \leq 0 \quad \forall\lambda.$$

The only way in which the causal curve can be closed is by connecting any initial point $(t_0\,,z_0\,,\phi_0)$ with $(t_0\,,z_0\,,\phi_0+\Delta)$. This automatically requires the existence of, at least one value of the affine parameter λ, say $\lambda = \lambda_\star$, where the timelike component of the tangent vector to the causal curve vanishes

$$\exists\lambda = \lambda_\star \quad \text{s.t.} \quad \left.\frac{dt}{d\lambda}\right|_{\lambda_\star} = 0\,.$$

It is clear that the only way to satisfy the causal character of the curve at $\lambda_\star$ is by having a vanishing tangent vector at that point, which contradicts the assumption of λ being an affine parameter. Thus we conclude that our discrete quotient is free of closed causal curves.

In order to identify the isometries of the quotient manifold, it is useful to describe AdS_3 as the $\mathrm{SL}(2,\mathbb{R})$ group manifold in terms of 2×2 matrices. An explicit global parametrization for this group manifold adapted to the action of the discrete quotient is given by

$$\hat{g} = e^{\phi\sigma_1}\ e^{z\sigma_3}\ e^{it\sigma_2}\,, \tag{2.15}$$

where σ_i are the standard Pauli matrices. Then, the metric in adapted coordinates (2.14) can be written as

$$g = \frac{l^2}{2}\mathrm{tr}(\hat{g}^{-1}d\hat{g})^2.$$

The isometry group is $\mathrm{SL}(2,\mathbb{R})\times\mathrm{SL}(2,\mathbb{R})$, and its action is given by left and right multiplication:

$$(h_L,h_R)\in \mathrm{SL}(2,\mathbb{R})\times\mathrm{SL}(2,\mathbb{R}):\ \hat{g}\to h_L\ \hat{g}\ h_R\ . \tag{2.16}$$

In this formulation, the discrete quotient under discussion is the identification

$$\hat{g}\sim e^{2\pi\sigma_1}\hat{g}\,, \tag{2.17}$$

which implies that $\phi\sim\phi+2\pi$. Notice that the identification is by an action of a hyperbolic element in the left $SL(2,R)$ and the trivial element of the right $SL(2,R)$.

The isometries of the quotient manifold are given in terms of the generators that commute with the action of the discrete quotient. Since the latter does not act on the right $\mathrm{SL}(2,\mathbb{R})$ factor, the isometry group will contain $\mathrm{SL}(2,\mathbb{R})$ besides the action along the quotient itself. Thus the isometries of the background (2.14) generate a $\mathrm{U}(1)\times\mathrm{SL}(2,\mathbb{R})$ group. Its generators, in the adapted coordinate system (2.13), are given in terms of the Killing vectors

$$\begin{aligned}
\xi &= \frac{1}{2}\frac{\partial}{\partial\phi}\,,\\
\chi_1 &= \frac{1}{2}\frac{\partial}{\partial t}\,,\\
\chi_2 &= \frac{1}{2}\tanh(2z)\cos(2t)\frac{\partial}{\partial t} + \frac{\cos 2t}{2\cosh(2z)}\frac{\partial}{\partial\phi} + \frac{1}{2}\sin(2t)\frac{\partial}{\partial z}\,,\\
\chi_3 &= -\frac{1}{2}\tanh(2z)\sin(2t)\frac{\partial}{\partial t} - \frac{\sin 2t}{2\cosh(2z)}\frac{\partial}{\partial\phi} + \frac{1}{2}\cos(2t)\frac{\partial}{\partial z}\,,
\end{aligned} \tag{2.18}$$

where $\{\chi_i=\xi_i^-\}$ satisfy the $\mathfrak{sl}(2,\mathbb{R})$ commutation relations

$$[\chi_1\,,\chi_2]=\chi_3\quad,\quad[\chi_3\,,\chi_1]=\chi_2\quad,\quad[\chi_2\,,\chi_3]=-\chi_1\ .$$

Compactification to AdS_2: The existence of an $\mathrm{SL}(2,\mathbb{R})$ isometry group suggests a close relationship between our orbifold (2.14) and AdS_2. This relation can be made precise by realizing that the metric (2.14) is an S^1 fibration over AdS_2. Indeed, we can rewrite (2.14) as

$$g = l^2\left(-\cosh^2(2z)\,dt^2 + dz^2 + (d\phi+\sinh(2z)\,dt)^2\right)\ . \tag{2.19}$$

Compactifying on ϕ now gives the metric

$$\begin{aligned} g_2 &= -\cosh^2 2z\, dt^2 + dz^2 \ , \\ A_1 &= \sinh 2z\, dt. \end{aligned} \tag{2.20}$$

The metric is precisely that of AdS_2, but there is also a constant electric field.[4] As we will see in Sec. 2.2.1, the two disconnected conformal boundaries of AdS_2 are also reflected in the boundary of the 3d space.

Supersymmetry: When considering the above construction in a supergravity context, it is important to analyze the supersymmetry preserved by the discrete identification. This was already discussed in [11] by explicit computation of the Killing spinors in the adapted coordinates (2.13). The conclusion of that paper was that the configuration (2.14) preserves one half of the spacetime supersymmetry. A much simpler way to get to the same conclusion is, once more, to think of AdS_3 as embedded in $\mathbb{R}^{2,2}$. The following discussion is based on the general discussion that will be presented in [17].

Killing spinors in this embedding space are just constant spinors ε_0 and they have two different chiralities. When decomposing the type IIB chiral spinors into tensor products of spinors in AdS_3, S^3 and a 4-torus, the Majorana spinors in AdS_3 transform in two different representations. Each of these is mapped to a different chiral sector in $\mathbb{R}^{2,2}$. The amount of supersymmetry preserved by the discrete identification is obtained by analyzing how many of the constant parallel spinors ε_0 remain invariant under the action of the generator of the discrete group (2.7). Infinitesimally, the latter condition is equivalent to [19, 20]

$$L_\xi \varepsilon_0 \equiv \nabla_\xi \varepsilon_0 + \frac{1}{4} \partial_{[m} \xi_{n]} \Gamma^{mn}\, \varepsilon_0 = 0 \ , \tag{2.21}$$

which gives rise to the algebraic constraint

$$\Gamma_{uvxy}\, \varepsilon_0 = \varepsilon_0 \ , \tag{2.22}$$

which is only satisfied by half of the components of the Killing spinor, since $(\Gamma_{uvxy})^2 = \mathbb{I}$ and $\mathrm{Tr}\, \Gamma_{uvxy} = 0$.

The above condition tells us that only the subset of parallel spinors in $\mathbb{R}^{2,2}$ with a positive chirality are left invariant after the action generated by (2.7). From the perspective of AdS_3, only one of the two inequivalent representations is not projected out by the quotient. Thus, we conclude our discrete quotient preserves one half of the supersymmetry, a conclusion that can also be reached by explicit computation.

2.2 Conformal boundary geometry

We seek the conformal boundary of our orbifold since we expect, a CFT living on it to give the holographic description of string theory on our space. A priori, there are two natural approaches to this problem, which are generically inequivalent. We could approach this in two ways: (a), we could

[4] The field is constant in the sense that the field strength of the U(1) connection is proportional to the AdS_2 volume form.

determine the conformal boundary of the discrete quotient manifold (2.14), or (b) we could study the quotient of the conformal boundary of AdS_3. As we will see that the discrete identification we are using induces a *conformal* transformation rather than an isometry of the AdS_3 boundary. Thus, approach (b) is not well defined here, but we will discuss the relevant transformations since they are useful later.

2.2.1 Conformal boundary of the quotient

Global AdS_3 has an $\mathbb{R}\times S^1$ cylinder as its conformal boundary, located at $\rho\to\infty$ in the coordinates (2.2). The map to coordinates adapted to the orbifold (2.13) is:

$$\begin{aligned}\cosh^2\rho &= \cosh^2 z\,\cosh^2\phi + \sinh^2 z\,\sinh^2\phi\,,\\ \tan\tau &= \frac{\tan t - \tanh z\tanh\phi}{1+\tanh z\tanh\phi\tan t}\,,\\ \tan\theta &= \frac{\tanh\phi\tan t - \tanh z}{\tanh\phi+\tanh z\tan t}\,.\end{aligned}\tag{2.23}$$

We see that the AdS_3 boundary at $\rho\to\infty$ can be reached by either taking $z\to\pm\infty$ or $\phi\to\pm\infty$ in the adapted coordinates.

To get some familiarity with the adapted coordinates, let us display global AdS_3 as a solid cylinder. Then, the equal z and equal t surfaces of (2.14) in the adapted coordinates are displayed in Figs. 1 and 2. An equal z section is a helical strip (actually a cylinder since the opposite ends of the strip are identified) which winds up the global cylinder. The boundary of the quotient consists of two such strips on the boundary of the global cylinder, with each strip being at $z=\infty$ or $z=-\infty$. It is easy to see why the original AdS_3 boundary splits into two pieces. The action of the orbifold makes ϕ a compact variable. So the region between the two strips on the boundary of the global cylinder is the locus of the points for which $\phi\to\pm\infty$.

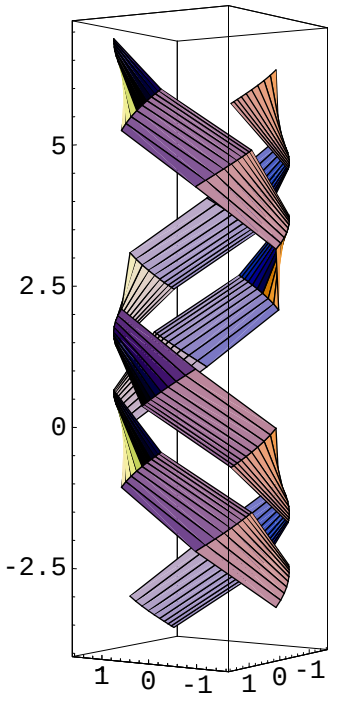

Figure 1: Equal z slices.

The metric on these conformal boundaries can be worked out using standard techniques. Let us consider the coordinate transformation

$$\sinh z = \tan\theta \qquad \theta\in\left(-\frac{\pi}{2},\frac{\pi}{2}\right)$$

bringing infinity to a finite distance . The metric of our discrete quotient (2.14) can be written as

$$g=\frac{l^2}{(\cos\theta)^2}\left((\cos\theta)^2(-(dt)^2+(d\phi)^2)+(d\theta)^2+4\sin\theta dt d\phi\right)\ .$$

It is then clear that the metric on both conformal boundaries, located at $\theta\to\pm\frac{\pi}{2}$ is given by

$$\tilde{g}=\pm dt d\phi\ ,\tag{2.24}$$

after a conformal rescaling.

The metric (2.24) is locally that of flat two dimensional space in lightcone coordinates. However, ϕ is an angular coordinate. Thus both conformal boundaries have closed lightlike curves. We will refer to such a geometry with a flat metric and one compact null direction as a *null cylinder*. We explained that from the AdS_2 fibration perspective the space also has two boundaries, but that they are timelike lines. The two points of view are reconciled by observing that in AdS_2 there is an electric field that dominates over the metric components at large z, explaining the light-like nature of the 3d boundary.

We can get some insight into such null cylinder geometries by examining the geometry of fixed z surfaces in the metric (2.14). The metric on any fixed z surface is

$$g = l^2(-dt^2 + d\phi^2 + 2\sinh(2z)\, dt d\phi) \ , \qquad (2.25)$$

where ϕ is periodically identified. In fact this metric is conformally related to a boosted version of the metric on a time-like cylinder swept out by t and ϕ at $z = 0$:

$$g = l^2(-dt_0^2 + d\phi_0^2) \ , \qquad (2.26)$$

where ϕ_0 is a circular direction with $\phi_0 \sim \phi_0 + 2\pi$. To see this, we boost (2.26) with a rapidity η to get the new coordinates

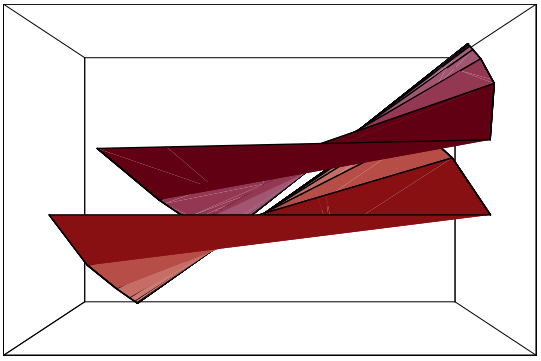

Figure 2: Equal t slices: The equal t sections, when displayed in global coordinates look like wedges that rotate in global AdS as t increases.

$$\tilde{t} = t_0 \cosh(\eta) - \phi_0 \sinh(\eta) \quad ; \quad \tilde{\phi} = -t_0 \sinh(\eta) + \phi_0 \cosh(\eta) \, . \qquad (2.27)$$

These new coordinates for the cylinder are identified as $(\tilde{t},\, \tilde{\phi}) \sim (\tilde{t},\, \tilde{\phi}) + 2\pi\,(-\sinh\eta,\, \cosh\eta)$. It is convenient to choose an adapted coordinate system in which the identification acts at a fixed time

$$\tau \equiv \tilde{t}\, \cosh\eta + \tilde{\phi}\, \sinh\eta = t_0 \quad ; \quad \beta \equiv -\tilde{t}\, \sinh\eta + \tilde{\phi} \cosh\eta \qquad (2.28)$$

in terms of which the identifications are $\beta \sim \beta + 2\pi \cosh(2\eta)$ at fixed τ. This leads to a metric

$$g = \frac{1}{\cosh^2(2\eta)}[-d\tau^2 + d\beta^2 + 2\sinh(2\eta)\, d\tau\, d\beta] \qquad (2.29)$$

This is conformal to the metric on fixed z slices (2.25). A further rescaling of coordinates

$$\tau \equiv \cosh(2\eta)\, t \quad ; \quad \beta \equiv \cosh(2\eta)\, \phi \qquad (2.30)$$

leads to the metric on the metric on the boosted cylinder

$$g = -dt^2 + d\phi^2 + 2\sinh(2\eta)\, dt\, d\phi \qquad (2.31)$$

exactly producing the metric (2.25) on the fixed z slices of our orbifold geometry. The radial coordinate z plays the role of the rapidity parameter in the boost. As $|z| \to \infty$ these metrics systematically approach the "null cylinder" of the conformal boundary.

2.2.2 Quotient of the conformal boundary

Alternatively, we can study how the generator of the discrete identification (2.7) acts on the original conformal boundary $\mathbb{R} \times S^1$ of AdS_3:

$$g = -(d\tau)^2 + (d\theta)^2 \,.$$

The isometry group $SO(2,2)$ in the bulk becomes the conformal group of the boundary metric. Its generators become conformal Killing vectors. One can write these generators explicitly, by rewriting J_{ab} in terms of the global coordinates (2.2) and evaluating them on the boundary:

$$\begin{aligned}
J_{01} &= \partial_\tau \\
J_{02} &= -(\cos\theta \sin\tau \partial_\tau + \cos\tau \sin\theta \partial_\theta) \\
J_{03} &= -\sin\theta \sin\tau \partial_\tau + \cos\tau \cos\theta \partial_\theta \\
J_{12} &= \cos\theta \cos\tau \partial_\tau - \sin\tau \sin\theta \partial_\theta \\
J_{13} &= \sin\theta \cos\tau \partial_\tau + \sin\tau \cos\theta \partial_\theta \\
J_{23} &= -\partial_\theta \,.
\end{aligned} \tag{2.32}$$

Therefore, the maximal compact subgroup of $SO(2,2)$ that is generated by $\{J_{01}\,, J_{23}\}$ is an isometry of the boundary metric, whereas the remaining generators are conformal Killing vectors. Indeed,

$$\left(\mathcal{L}_{J_{0k}+iJ_{1k}} g\right)_{ab} = 2\Omega_k g_{ab} \,, \tag{2.33}$$

where g_{ab} stands for the boundary metric and $(\Omega_2, \Omega_3) = e^{i\tau}(\cos\theta\,, \sin\theta)$.

This analysis shows that the generator of our orbifold (2.7) is not an isometry of the boundary metric, but it is a conformal Killing vector. Thus it is not clear what a discrete quotient of the AdS_3 boundary by this generator should mean. For later reference, the explicit expression for the generator of this discrete action on $\mathbb{R} \times S^1$ is

$$\xi_{\rho\to\infty} = -\frac{1}{2}\sin(\tau-\theta)\,(\partial_\tau - \partial_\theta) \,. \tag{2.34}$$

Some comments are in order:

- If we forget about the factor $\sin(\tau-\theta)$, the identification would certainly generate a closed lightlike direction, matching our previous conclusion.
- The action on the conformal boundary $\mathbb{R} \times S^1$ has fixed points located at $\tau = \theta (\mathrm{mod}\, \pi)$. This may seem surprising because our bulk analysis allowed us to write the generator as $\partial/\partial\phi$ everywhere, both in the bulk and the boundary, which shows there are no fixed points. However, this misses the fixed point at $\phi \to \pm\infty$. From (2.23), it is clear that $\phi \to \pm\infty$ corresponds to $\tau = \theta$.

In summary, we have established that the conformal boundary of our orbifold consists of two null cylinders. In Sec. 4.2.2 we will explore the possibility of directly orbifolding the dual to AdS_3 by the above discrete conformal transformation to generate the dual to our orbifold.

2.3 Geodesics

Geodesics extremize the length of curves connecting two points. For a smooth curve $x^\mu(\lambda)$, the length S is

$$S = \int d\lambda \sqrt{|g_{\mu\nu} \frac{dx^\mu}{d\lambda} \frac{dx^\nu}{d\lambda}|} \,. \tag{2.35}$$

The problem is identical to the extremization of the action in Lagrangian particle mechanics. In fact, with affine parameterization, the geodesic equations can be obtained by variation of a simpler Lagrangian

$$L = g_{\mu\nu} \frac{dx^\mu}{d\sigma} \frac{dx^\nu}{d\sigma} \,, \tag{2.36}$$

where σ is now the affine parameter. For the metric in (2.14), this yields (we have set $l = 1$)

$$L = -\dot{t}^2 + \dot{\phi}^2 + \dot{z}^2 + 2\sinh(2z)\dot{\phi}\dot{t} \,, \tag{2.37}$$

where the dots stand for derivatives with respect to the affine parameter. Since the Lagrangian is independent of both t and ϕ, we have the conserved momenta:

$$\begin{aligned} P_t &= -2\dot{t} + 2\sinh(2z)\dot{\phi} = E \,, \\ P_\phi &= 2\dot{\phi} + 2\sinh(2z)\dot{t} = m \,, \end{aligned} \tag{2.38}$$

which imply

$$\begin{aligned} \dot{t} &= \frac{m\sinh(2z) - E}{2\cosh^2(2z)} \,, \\ \dot{\phi} &= \frac{E\sinh(2z) + m}{2\cosh^2(2z)} \,. \end{aligned} \tag{2.39}$$

In addition, the Hamiltonian H is equal to the Lagrangian L in our case and therefore the Hamiltonian constraint is

$$-\dot{t}^2 + \dot{\phi}^2 + \dot{z}^2 + 2\sinh(2z)\dot{\phi}\dot{t} = k \tag{2.40}$$

where we can choose the affine parameterization such that $k = -1, 0, 1$ for time-like, null and space-like geodesics respectively. From this we obtain

$$\dot{z} = \sqrt{k + \frac{E^2 - m^2}{4\cosh^2(2z)} - Em\frac{\sinh(2z)}{2\cosh^2(2z)}} \tag{2.41}$$

For generic values of the constants of motion E and m, this equation admits the following solutions:

$$\begin{aligned} k = 0 \qquad & \sinh(2z) = \frac{E^2 - m^2}{2mE} - \frac{(\sigma_0 - E \cdot m\sigma)^2}{2Em} \\ k = -1 \qquad & \sinh(2z) = -\frac{E \cdot m}{4} + \frac{1}{2}\cos(\sigma_0 - 2\sigma)\sqrt{E^2 - m^2 - 4 + (E \cdot m/2)^2} \\ k = 1 \qquad & \sinh(2z) = \frac{1}{2}\sinh(2\sigma + \sigma_0)\sqrt{E^2 - m^2 + 4 - (E \cdot m/2)^2} + \frac{E \cdot m}{4} \end{aligned} \tag{2.42}$$

Whenever $E = 0$, $m = 0$ or both, some of the previous solutions become singular, and so these cases have to be dealt with separately. Notice that from the square of equation (2.41), whenever

$E = m = 0$, timelike geodesics ($k = -1$) do not exist, and we are left with the trivial solution $z = z_0$, $t = t_0$ and $\phi = \phi_0$, or the spacelike geodesic ($k = 1$), $z = \pm\sigma + z_0$, $t = t_0$ and $\phi = \phi_0$. If we keep $E = 0$, but consider non-vanishing angular momentum, the solution can be obtained from the appropriate limit in (2.42). Such geodesics are space-like. Actually, if m is an integer, they only make sense for $m = 0, 1, 2$. For example, for $m = 2$ the solution is given by

$$\sinh 2z = Ce^{2\eta\sigma} \quad , \quad \eta = \pm \, . \tag{2.43}$$

If the angular momentum vanishes ($m = 0$), but we consider non-vanishing energy, one can find the lightlike geodesic

$$\sinh\, 2z = \eta \, E \, \sigma + \sigma_0 \, . \tag{2.44}$$

The spacelike solutions can be obtained from the corresponding limit in (2.42). Among the timelike ones, if $\dot{z} \neq 0$, the solutions only exist for $|E| > 2$. If $z = z_0$, then we can allow $|E| \geq 2$, and the solutions are given by $t = -\frac{2}{E}\sigma + t_0$ and $\phi = \sqrt{1 - 4/E^2}\sigma + \phi_0$. Note that for $E^2 = m^2$, one can find lightlike geodesics consisting of constant $z = z_0$, and linear dependences in the affine parameter both for t and ϕ. Finally, there are timelike geodesics at any constant z and ϕ (this is easily seen by solving $\dot{\phi} = \dot{z} = 0$). These geodesics descend from trajectories in global AdS that spiral around the origin. The spiral is "unwound" by the twisted coordinate system (2.13) that we have chosen from the perspective of the embedding in global AdS (see Fig. 2).

It is interesting to study which geodesics causally connect the two boundaries at $z = \pm\infty$. The lightlike geodesics ($k = 0$) written in (2.42), do not connect the two boundaries. Indeed, these are parabolas, so the best that we can do is to arrange initial conditions such that the geodesic starts at one boundary and gets as close as we want to the second conformal boundary. On the other hand, the lightlike geodesics with vanishing angular momentum in (2.44) provide a causal connection between the two boundaries. We can find the orbit in the $\{t, z\}$ plane in this case, and compute the coordinate time required for the null particles to go from $z \to -\infty$ to the other boundary at $z \to \infty$. The result is given by the finite expression

$$t(z = +\infty) - t(z = -\infty) = -\eta\frac{\pi}{2} \, . \tag{2.45}$$

Timelike geodesics show an oscillatory behavior and they do not connect both boundaries. In sum, the only way to connect both boundaries with a geodesic is to use the null trajectory described above, or to consider unphysical extreme initial quantum numbers such as $E \to \infty$ and $m =$ constant.

2.4 Excursions in the complex coordinate plane

While discussing holography for our orbifold, we will see that the symmetries and structure of the complexified manifold play an important role. First of all, notice that while our metric

$$ds^2 = -dt^2 + dz^2 + d\phi^2 + 2\,\sinh(2z)\, dt\, d\phi \tag{2.46}$$

is non-singular everywhere for real ϕ, z and t, the determinant

$$\det g = -\cosh^2(2z) \tag{2.47}$$

vanishes at $z = i\pi/4$. It is not apparent at this point that this singularity in the complex coordinate plane should play any role in the physics, but as we will see later, this singularity make a crucial appearance in the analysis of holography.

For later purposes it will be very useful to understand the symmetries of (2.46) as a metric on the space of complexified coordinates.

Discrete symmetries in the complex coordinate plane: In the global parametrization (2.2), the following discrete complex transformations of coordinates leave invariant points of the quadric defining AdS_3 in $\mathbb{R}^{2,2}$ (2.1):

$$\rho \to \rho + i\,\pi \quad , \quad \tau \to \tau + \pi \quad , \quad \theta \to \theta + \pi \ , \tag{2.48}$$

In the coordinate system adapted to our orbifold (2.13), there is a richer structure due to the combination of trigonometric and hyperbolic functions in the parametrization. Three discrete complex coordinate transformations that leave the embedding invariant are

$$z \to z \quad , \quad t \to t + \pi \quad , \quad \phi \to \phi + i\,\pi \ , \tag{2.49}$$

$$z \to z + i\,\pi \quad , \quad t \to t + \pi \quad , \quad \phi \to \phi \ , \tag{2.50}$$

$$z \to z + i\,\pi \quad , \quad t \to t \quad , \quad \phi \to \phi + i\,\pi \ . \tag{2.51}$$

These complex transformations of coordinates map real physical points on the orbifold to themselves. Later we will see that the solutions to the wave equation on our orbifold will reflect this symmetry in complex coordinate plane.

Motions through the complex coordinate plane: In addition, certain discrete complex coordinate transformations generate transformations between real physical points in the orbifold. First, we show a transformation connecting the two components of the conformal boundary of the spacetime. Consider (2.23) which relates the global and adapted coordinates. We are interested in boundary points, namely $z \to \pm\infty$. In global coordinates this amounts to $\rho \to \infty$ in the first of the equations (2.23). The second and third equations can then be rewritten in terms of a sign η corresponding to the boundary at $z \to \eta\infty$:

$$\begin{aligned} \tan\tau &= \frac{\tan t - \eta \tanh\phi}{1 + \eta \tanh\phi \tan t} \,, \\ \tan\theta &= \frac{\tanh\phi \tan t - \eta}{\tanh\phi + \eta \tan t} \,. \end{aligned} \tag{2.52}$$

Now, consider the discrete transformation

$$t = t' + \frac{\pi}{2} \quad , \quad \phi = \phi' + i\,\frac{\pi}{2} \ , \tag{2.53}$$

defined on the boundary $z \to \infty$. Taking the expressions (2.52) with $\eta = +1$, and using the transformations (2.53), we find the description of a point in global AdS_3 coordinates sitting at

$\rho \to \infty$ with (τ', θ') given by

$$\begin{aligned} \tan\tau' &= \frac{\tan t' + \tanh\phi'}{1 - \tanh\phi' \tan t'} \,, \\ \tan\theta' &= \frac{\tanh\phi' \tan t' + 1}{\tanh\phi' - \tan t'} \,. \end{aligned} \tag{2.54}$$

But this is precisely the description of a point in the second boundary $z \to -\infty$ obtained by evaluating (2.52) with $\eta = -1$. Therefore the complex transformations (2.53) map points in the boundary $z \to \infty$ to points in the second boundary at $z \to -\infty$.

In fact, (2.53) can be extended to a complex transformation mapping real points on the orbifold for all $z > 0$ to corresponding points at $z < 0$. Keeping in mind the relation

$$\cosh^2\rho = \cosh^2 z \, \cosh^2\phi + \sinh^2 z \, \sinh^2\phi \,. \tag{2.55}$$

let us extend the transformation (2.53) by the following action on z

$$z = z' + i\,\frac{\pi}{2} \,. \tag{2.56}$$

This transformation preserves $\cosh^2\rho = \cosh^2\rho'$. Since $\tanh z = -(1/\tanh z')$, the point in global AdS_3 described by (t', ϕ', z') is given by

$$\begin{aligned} \tan\tau' &= \frac{\tanh z' \tan t' + \tanh\phi'}{1 - \tanh z' \tanh\phi' \tan t'} \,, \\ \tan\theta' &= \frac{\tanh\phi' \tan t' + \tanh z'}{\tanh\phi' - \tanh z' \tan t'} \,. \end{aligned} \tag{2.57}$$

Thus, we can identify (t', ϕ', z') with $(t, \phi, -z)$ by explicitly evaluating (2.23).

We will see that these discrete transformations in the complex coordinate plane that map real physical points to each other have an intimate relation to the structure of holographic duality in the orbifold.

3. Scalar field theory

Since the AdS orbifold constructed in the previous section has two boundaries we expect that the dual field theory will take a novel form. It could be a product of two independent CFTs, or the two components could be identified or entangled. The first step in understanding both bulk and boundary dynamics is to study scalar field theory in the background (2.14) with the orbifold identification $\phi \sim \phi + 2\pi$. In Lorentzian AdS spaces we expect a spectrum of normalizable modes corresponding to states in the dual CFT and non-normalizable modes corresponding to sources [15]. We will find a basis of such mode solutions and use them to infer facts about the structure of the CFT.

The wave equation for a massive scalar is

$$(\Box - \mu^2)\Psi = 0 \tag{3.1}$$

where μ includes the effects of a curvature coupling, if there is one, since the curvature is constant in our orbifold. For the metric (2.14), this becomes,

$$\left\{-\frac{\partial^2}{\partial t^2}+\cosh^2(2z)\,\frac{\partial^2}{\partial z^2}+\frac{\partial^2}{\partial\phi^2}+2\sinh(2z)\,\frac{\partial^2}{\partial t\partial\phi}+\sinh(4z)\,\frac{\partial}{\partial z}-\mu^2\cosh^2(2z)\right\}\Psi=0 \qquad (3.2)$$

3.1 Unitary representations of $SL(2,R)$ and fluctuating states

Fluctuating states on the orbifold spacetime should lie in a unitary representation of the isometry group $\mathrm{SL}(2,\mathbb{R})\times\mathrm{U}(1)$. Following [15] and references therein we should look for a highest weight representation of $\mathrm{SL}(2,\mathbb{R})$. To this end, define a new basis for the $\mathfrak{sl}(2,\mathbb{R})$ generators in (2.18) as

$$\begin{aligned}
\mathcal{L}_0 &= i\chi_1=\frac{i}{2}\frac{\partial}{\partial t}\\
\mathcal{L}_+ &= \chi_2-i\chi_3=\frac{e^{2it}}{2}\left[\tanh(2z)\frac{\partial}{\partial t}+\frac{1}{\cosh(2z)}\frac{\partial}{\partial\phi}-i\frac{\partial}{\partial z}\right]\\
\mathcal{L}_- &= -(\chi_2+i\chi_3)=-\frac{e^{-i2t}}{2}\left[\tanh(2z)\frac{\partial}{\partial t}+\frac{1}{\cosh(2z)}\frac{\partial}{\partial\phi}+i\frac{\partial}{\partial z}\right],
\end{aligned} \qquad (3.3)$$

in terms of which the $\mathfrak{sl}(2,\mathbb{R})$ algebra is $[\mathcal{L}_0,\mathcal{L}_\pm]=\mp\mathcal{L}_\pm$ and $[\mathcal{L}_+,\mathcal{L}_-]=2\mathcal{L}_0$. Highest weight states satisfy $\mathcal{L}_+|h\rangle=0$ and $\mathcal{L}_0|h\rangle=h|h\rangle$. A complete highest weight representation is constructed as $\mathcal{L}_-^n|h\rangle$ for $n\geq 0$. In such a highest weight representation the $\mathfrak{sl}(2,\mathbb{R})$ Casimir is given by

$$2\mathcal{L}^2=2\mathcal{L}_0^2-(\mathcal{L}_+\mathcal{L}_-+\mathcal{L}_-\mathcal{L}_+)=2h(h-1) \qquad (3.4)$$

In terms of the explicit differential operators in (3.3), it is easy to show that the Casimir equation can be written as

$$4\mathcal{L}^2\psi=\Box\psi=4h(h-1)\psi \qquad (3.5)$$

so a solution to the wave equation (3.2) that is in a highest weight representation of the isometries satisfies

$$\mu^2=4h(h-1) \quad\Longrightarrow\quad h_\pm=\frac{1}{2}\pm\frac{1}{2}\sqrt{1+\mu^2} \qquad (3.6)$$

Highest weight states solve the equation

$$\mathcal{L}_+\Psi(t,z,\phi)\equiv\mathcal{L}_+\psi(t,z)e^{im\phi}=0 \quad;\quad \mathcal{L}_0\Psi(t,z,\phi)\equiv\mathcal{L}_0\psi(t,z)e^{im\phi}=h\psi(t,z)e^{im\phi} \qquad (3.7)$$

where we have have Fourier transformed in ϕ since $\xi=(i/2)(\partial/\partial\phi)$ is an isometry. The second equation yields $\Psi=\tilde{\psi}(z)e^{-2iht}e^{im\phi}$ and the remaining first order differential equation is easily solved to give

$$\Psi(t,z,\phi)=C\left[\cosh(2z)\right]^{-h}e^{m\tan^{-1}[\tanh(z)]}\,e^{-2iht}\,e^{im\phi} \qquad (3.8)$$

where C is a normalization constant.

We first examine the behavior of (3.8) at the orbifold boundaries $z\to\pm\infty$. In this limit $\tan^{-1}[\tanh(z)]\to\pm\pi/4$, and so that as $z\to\pm\infty$, $|\Psi|\to 0$ if $h>0$ and $|\Psi|\to\infty$ if $h<0$. For $\mu^2>0$, normalizable modes arise from h_+ and non-normalizable modes from h_-. When $m=0$ the normalizable highest weight state is a lump localized around $z=0$. When $m<0$ ($m>0$) the state

is a lump is localized at some $z_0 < 0$ ($z_0 > 0$) (see Fig. 3). The non-normalizable modes diverge when $z \to \pm\infty$, but they too are asymmetric when $m \neq 0$. For negative (positive) m, these modes grown much faster in the region $z < 0$ ($z > 0$). This behavior has the consequence that the physics of modes with positive m is largely concentrated at positive z while the physics of negative m is largely concentrated at negative z.

A complete highest weight representation is obtained by acting on (3.8) with the operator $\mathcal{L}_-^n$. The descendants are characterized conveniently in terms of

$$\Psi_h(t\,,\phi\,,z) = e^{-2iht}\,e^{im\phi}\,\Psi_h(z) \equiv e^{-2iht}\,e^{im\phi}\,\Big(\cosh 2z\Big)^{-h}\,e^{m\tan^{-1}[\tanh(z)]} \quad \forall h\ .$$

Since $\Psi_h'(z) = \Psi_{h+1}(z)\,(-2h\sinh 2z + m)$,

$$\mathcal{L}_-\Psi_h(t\,,\phi\,,z) = i\,(2h\sinh 2z - m)\,\Psi_{h+1}(t\,,\phi\,,z) \quad \forall h\ . \tag{3.9}$$

In general, $\mathcal{L}_-^n\Psi_h(t\,,\phi\,,z) = g(n,z)\Psi_{h+n}(t\,,\phi\,,z)$. We will derive $g(n,z)$ in the next subsection.

3.2 Normalizable vs. non-normalizable modes and analytic structure

The non-normalizable modes which are necessary for the AdS/CFT correspondence are expected to be in a mixture of $SL(2,R)$ representations [15] and so it is more convenient to directly solve for them from the wave equation (3.2). On the way this will also give us the function $g(n,z)$ for the descendant normalizable states.

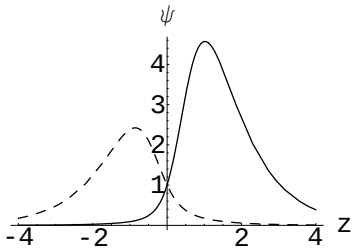

Figure 3: Mode solutions: The dashed solution corresponds to $m < 0$, whereas the solid one corresponds to $m > 0$.

We start with the ansatz

$$\Psi(t,z,\phi) = e^{-i\omega t + im\phi}\psi(z)\ . \tag{3.10}$$

Inserting this into (3.2), one obtains:

$$\cosh^2(2z)\frac{d^2\psi}{dz^2} + \sinh(4z)\frac{d\psi}{dz} + \Big(\omega^2 - m^2 + 2\omega m\sinh(2z) - \mu^2\cosh^2(2z)\Big)\psi = 0\ . \tag{3.11}$$

Consider the change of variables

$$\psi(z) \;=\; \Big(\cosh 2z\Big)^b\,e^{a\tan^{-1}[\tanh(z)]}\,\chi(z) \tag{3.12}$$

$$y \;=\; \frac{1}{2}(1 + i\sinh 2z)\,, \tag{3.13}$$

The function $\chi(z)$ then satisfies the hypergeometric equation

$$y(1-y)\frac{d^2\chi}{dy^2} + \Big(C - (1+A+B)y\Big)\frac{d\chi}{dy} - AB\chi = 0 \tag{3.14}$$

provided

$$4b^2 - \omega^2 + m^2 - a^2 + (4ba + 2\omega m)i = 0.$$

This equation is solved by $b = \mp\frac{\omega}{2}$ and $a = \pm m$ – either choice of signs will give identical solutions. So from now on we choose the upper signs. The constant parameters A, B and C appearing in (3.14) are determined in terms of $\{m\,, \omega\,, \mu^2\}$ by:

$$\begin{aligned} A &= -\frac{\omega}{2} + \frac{1}{2} - \frac{1}{2}\sqrt{1+\mu^2} = -\frac{\omega}{2} + h_- \\ B &= -\frac{\omega}{2} + \frac{1}{2} + \frac{1}{2}\sqrt{1+\mu^2} = -\frac{\omega}{2} + h_+ \\ C &= 1 - \Big(\frac{\omega + im}{2}\Big), \end{aligned} \tag{3.15}$$

In order to determine the normalizable and non-normalizable solutions of (3.14), we need to determine the asymptotic behavior of the solutions as $z \to \pm\infty$. For this reason, it is most convenient to write the solution in terms of hypergeometric functions with arguments $1/y$:

$$\chi(z) = c_1\, y^{-A}{}_2F_1(A, A-C+1; A-B+1; \frac{1}{y}) + c_2\, y^{-B}{}_2F_1(B, B-C+1; B-A+1, \frac{1}{y}) \tag{3.16}$$

The solution is written as a sum of two independent solutions of the hypergeometric equation. This is a convenient basis of solutions to isolate the normalizable and non-normalizable solutions.

Asymptotics As $z \to \infty$, $\frac{1}{y} \to 0$, and the hypergeometric functions in (3.16) approach 1. Thus

$$\chi \to c_1\, y^{-A} + c_2\, y^{-B} \tag{3.17}$$

For the full solution $\Psi(t, \phi, z)$ in (3.10), using (3.12), this implies

$$\Psi(t, \phi, z) \to e^{-i\omega t + im\phi}(c_1\,(e^{2z})^{-h_-} + c_2\,(e^{2z})^{-h_+}) \tag{3.18}$$

As $z \to -\infty$, the asymptotic behavior is

$$\Psi(t, \phi, z) \to e^{-i\omega t + im\phi}(c_1\,(e^{-2z})^{-h_-} + c_2\,(e^{-2z})^{-h_+}) \tag{3.19}$$

Hence the solution with coefficient c_2 decays at both boundaries while the solutions multiplying c_1 grows at both boundaries and is non-normalizable.

3.2.1 Normalizable solutions

We seek a basis for the fluctuating normalizable mode solutions for the scalar field. Candidates are given by the modes that decay at infinity:

$$\Psi_{\rm norm}(t, \phi, z) = e^{-i\omega t + im\phi} e^{m\tan^{-1}(\tanh(z))} (\cosh(2z))^{-\frac{\omega}{2}}\; y^{(\frac{\omega}{2} - h_+)}\; {}_2F_1(-\frac{\omega}{2} + h_+, h_+ + i\frac{m}{2}; 2h_+; \frac{1}{y}) \tag{3.20}$$

We have already displayed a suitable basis of modes via the analysis of unitary SL(2,R) representations given above. However we will see that the same quantized spectrum of solutions arises from (3.20) by requiring that the mode solutions should be single valued in the complex z plane. Presumably this requirement is necessary for unitarity.

To this end, let us study the behavior of (3.20) as $y \to 0$ or, equivalently, as $z \to i\pi/4$. In Sec. 2.4 we noted that $z = i\pi/4$ is a location in the complex coordinate plane at which the determinant of the metric (2.14) vanishes; namely this is a singular point in the complex coordinate plane. Using the transformation formula

$$
\begin{aligned}
{}_2F_1(\tilde{a},\tilde{b};\tilde{c};\frac{1}{y}) = \frac{\Gamma(\tilde{c})\Gamma(\tilde{b}-\tilde{a})}{\Gamma(\tilde{b})\Gamma(\tilde{c}-\tilde{a})}(-\frac{1}{y})^{-\tilde{a}}{}_2F_1(\tilde{a},1-\tilde{c}+\tilde{a};1-\tilde{b}+\tilde{a};y) \\
+ \frac{\Gamma(\tilde{c})\Gamma(\tilde{a}-\tilde{b})}{\Gamma(\tilde{a})\Gamma(\tilde{c}-\tilde{b})}(-\frac{1}{y})^{-\tilde{b}}{}_2F_1(\tilde{b},1-\tilde{c}+\tilde{b};1-\tilde{a}+\tilde{b};y)
\end{aligned}
$$

we find

$$
\begin{aligned}
\Psi \quad &\sim (-1)^{(\omega/2-h_+)}\frac{\Gamma(2h_+)\Gamma(\frac{\omega+im}{2})}{\Gamma(h_+ + \frac{im}{2})\Gamma(h_+ + \frac{\omega}{2})}{}_2F_1(-\frac{\omega}{2}+h_+,-\frac{\omega}{2}+h_-;1-\frac{\omega+im}{2};y) \\
&+ (-1)^{-(h_+ + im/2)}\frac{\Gamma(2h_+)\Gamma(-\frac{\omega+im}{2})}{\Gamma(-\frac{\omega}{2}+h_+)\Gamma(h_+ - i\frac{m}{2})}\, y^{(\frac{\omega+im}{2})}{}_2F_1(h_+ + i\frac{m}{2}, h_- + i\frac{m}{2};1+i\frac{m}{2}+\frac{\omega}{2};y)\ .
\end{aligned}
\tag{3.21}
$$

Thus, the second term in (3.21) gives rise to a multivalued function in the complex z-plane.[5] Requiring a single valued scalar wave function forces us to require the vanishing of the second coefficient in (3.21). This is achieved by

$$
-\frac{\omega}{2} + h_+ = -n \qquad n \in \mathbb{Z}^+ \cup \{0\}\ , \tag{3.22}
$$

which ensures that $\Gamma(-\frac{\omega}{2}+h_+)$ has a vanishing or negative integer argument which makes it diverge. Thus, by looking at (3.20) and its complex conjugate, we find that the allowed states have energies (eigenvalues of $i\partial/\partial t$)

$$
E_n = \pm 2(h_+ + n) \qquad n \in \mathbb{Z}^+ \cup \{0\}\ . \tag{3.23}
$$

This quantization condition was also obtained from the analysis of highest weight representations of the isometry group in the previous subsection. Notice that the spectrum is entirely independent of the angular momentum quantum number m. It is intriguing that requiring regularity of the solutions at a point the complex z plane where the complexified metric degenerates has correctly selected the quantized spectrum of modes expected from SL(2,R) representation theory.

With this quantization the positive energy solutions in (3.20) become

$$
\begin{aligned}
\Psi = e^{-i(2h_+ + 2n)t + im\phi}e^{m\tan^{-1}(\tanh(z))}(\cosh(2z))^{-(h_+ + n)}\ \Big(\frac{1}{2}(1+i\sinh(2z))\Big)^n \\
\times {}_2F_1(-n, h_+ + i\frac{m}{2}; 2h_+; \Big(\frac{1}{2}(1+i\sinh(2z))\Big)^{-1})
\end{aligned}
\tag{3.24}
$$

We can write the hypergeometric function appearing in this equation in terms of Jacobi polynomials by using

$$
{}_2F_1(-n,\alpha+\beta+n+1;\alpha+1;x) = \frac{n!\Gamma(2h_+)}{\Gamma(2h_+ + n)}P_n^{(\alpha,\beta)}(1-2x) \tag{3.25}
$$

[5]The nature of the cut is somewhat different when $m = 0$ as opposed to $m \neq 0$.

where $P_n^{(\alpha,\beta)}$ are the Jacobi polynomials defined as:

$$P_n^{(\alpha,\beta)}(u) = \frac{\Gamma(\alpha+n+1)}{n!\Gamma(\alpha+\beta+n+1)} \sum_{k=0}^{n} \binom{n}{k} \frac{\Gamma(\alpha+\beta+k+n+1)}{2^k\Gamma(\alpha+k+1)} (u-1)^k \ . \tag{3.26}$$

Using $\alpha = 2h_+ - 1$ and $\beta = -h_+ - n + i\frac{m}{2}$, (3.24) becomes

$$\begin{aligned}\Psi_n \ = \ & e^{-i(2h_++2n)t+im\phi} e^{m\tan^{-1}(\tanh(z))} (\cosh(2z))^{-(h_++n)} \\ & \times \frac{\Gamma(2h_+)}{\Gamma(h_+ + i\frac{m}{2})} \sum_{k=0}^{n} \binom{n}{k} \frac{\Gamma(h_+ + i\frac{m}{2} + k)}{\Gamma(2h_+ + k)} (-1)^k \Big(\frac{1}{2}(1 + i\sinh(2z))\Big)^{n-k}\end{aligned} \tag{3.27}$$

Earlier we derived the fluctuating states by analyzing a highest weight representation of the isometries. The above analysis completes this derivation by giving an explicit form for the states as can checked from the equation $\Psi_n = \mathcal{L}_-^n \Psi_h$ where Ψ_h was defined in (3.8). Thus we see that requiring analyticity of the scalar wavefunctions in the complex coordinate plane is equivalent here to requiring that they transform in a unitary representation.

3.2.2 Non-normalizable solution

The non-normalizable part of the solution (3.16) is

$$\Psi_{\rm non-norm} = e^{-i\omega t+im\phi} e^{m\tan^{-1}(\tanh(z))} (\cosh(2z))^{-\frac{\omega}{2}} \ y^{(\frac{\omega}{2}-h_-)} \ {}_2F_1(-\frac{\omega}{2}+h_-, h_- + i\frac{m}{2}; 2h_-; \frac{1}{y}) \tag{3.28}$$

The non-normalizable modes in AdS are related to sources in the dual field theory and hence should not be quantized [15]. These modes can also be thought of as a momentum space representation of the bulk-boundary propagator. Notice that the non-normalizable character of a mode is not changed by adding any normalizable modes to it. This ambiguity in the selection of a basis of non-normalizable modes is related to the selection of a vacuum state for the spacetime and for the dual field theory [15, 4, 42]. A distinguished set of non-normalizable modes can be selected by requiring that they have regular behavior as $y \to 0$ or $z \to i\pi/4$, namely that they are single valued in the complex coordinate plane just like the normalizable ones.

Using the transformation formulae for hypergeometric functions we find, as a function of y,

$$\begin{aligned}\Psi_{\rm non-norm} \ & \sim (-1)^{-\omega/2+h_-} \frac{\Gamma(2h_-)\Gamma(\frac{\omega+im}{2})}{\Gamma(h_- + \frac{im}{2})\Gamma(h_- + \frac{\omega}{2})} {}_2F_1(-\frac{\omega}{2}+h_-, -\frac{\omega}{2}+h_+; 1-\frac{\omega+im}{2}; y) \\ & + (-1)^{h_-+im/2} \frac{\Gamma(2h_-)\Gamma(-\frac{\omega+im}{2})}{\Gamma(-\frac{\omega}{2}+h_-)\Gamma(h_- - i\frac{m}{2})} \ y^{(\frac{\omega+im}{2})} {}_2F_1(h_- + i\frac{m}{2}, h_+ + i\frac{m}{2}; 1 + i\frac{m}{2} + \frac{\omega}{2}; y) \ .\end{aligned} \tag{3.29}$$

The second term again implies a cut in the complex z plane starting from $y = 0$. For special values of ω, namely $\omega = -2h_- - n, \quad n = 0, 1, 2, \cdots$ the second term vanishes, but we need to include non-normalizable modes for all ω as discussed above. Notice, however, that for general ω the cuts appearing in (3.29) are identical in form to the cuts in the normalizable modes (3.21). Therefore, we will be able to cancel the cuts in (3.29) by adding a suitable linear combination of normalizable

modes. Indeed, the following combination of non-normalizable and normalizable modes is regular at the origin:

$$\Psi^{\rm regular}_{\rm non-norm} = \Psi_{\rm non-norm} - (-1)^{\nu}\frac{\Gamma(2h_-)\Gamma(-\frac{\omega}{2}+h_+)\Gamma(h_+-\frac{im}{2})}{\Gamma(2h_+)\Gamma(-\frac{\omega}{2}+h_-)\Gamma(h_--\frac{im}{2})}\Psi_{norm} \tag{3.30}$$

where $\nu = h_+ - h_-$ and $\Psi_{\rm non-norm}$ and $\Psi_{\rm norm}$ are as in (3.28) and (3.20).

3.2.3 The case of integer $\nu = \mathbf{h_+ - h_-} = \sqrt{\mathbf{1+\mu^2}}$ and a slightly different approach

Perhaps a simpler way to obtain the basis of normalizable and non-normalizable solutions discussed here is to start by picking the regular solution to (3.14) near $y = 0$. For a generic ω, this solution will be non-normalizable. However, for certain quantized frequencies, the solution should become normalizable. The general solution to (3.14) is given by

$$\chi(y) = c_1\, F(A,B;C;y) + c_2\, y^{1-C}F(A-C+1,B-C+1;2-C;y) \tag{3.31}$$

where $A,\ B$ and C are given in (3.15). For this solution to be regular at $y = 0$, we need the second term to be absent, *i.e.* $c_2 = 0$. Then, starting with the regular solution,

$$\chi(y) = F(-\frac{\omega}{2}+h_-,-\frac{\omega}{2}+h_+;1-\Big(\frac{\omega+im}{2}\Big),y) \tag{3.32}$$

we use the transformation formula (3.21) to determine its behavior near $y = \infty$:

$$\begin{aligned}\chi(y) = &\frac{\Gamma\left(1-\left(\frac{\omega+im}{2}\right)\right)\Gamma(h_+-h_-)}{\Gamma(-\frac{\omega}{2}+h_+)\Gamma(h_+-\frac{im}{2})}(-y)^{-\frac{\omega}{2}+h_-}F(-\frac{\omega}{2}+h_-,h_-+\frac{im}{2};2h_-;\frac{1}{y})\\ &+\frac{\Gamma\left(1-\left(\frac{\omega+im}{2}\right)\right)\Gamma(h_--h_+)}{\Gamma(-\frac{\omega}{2}+h_-)\Gamma(h_--\frac{im}{2})}(-y)^{-\frac{\omega}{2}+h_+}F(-\frac{\omega}{2}+h_+,h_++\frac{im}{2};2h_+;\frac{1}{y})\end{aligned}$$

The first term corresponds to the non-normalizable piece and for $-\frac{\omega}{2}+h_+ = -n$, where n is a non-negative integer, $\Gamma(-\frac{\omega}{2}+h_+)$ in the denominator has a pole, implying that for these particular quantized frequencies, the solution only has a normalizable piece. This normalizable solution as well as the quantization condition on ω is, of course, the same as what we obtained earlier in (3.20). Also, for a generic ω, it is easy to see that (3.32) is precisely the linear combination (3.30) which is non-normalizable and regular at the origin.

However, this analysis and our previous discussions break down when $\nu = h_+ - h_-$ is an integer. In this case, the transformation formula (3.21) is not valid. In fact, we then use the more complicated formula

$$\begin{aligned}\chi(y) = F(A,B;C;y) = \frac{\Gamma(C)(-y)^{-B}}{\Gamma(B)\Gamma(C-A)}\sum_{n=0}^{\infty}\frac{(A)_{n+\nu}(1-C+A)_{n+\nu}}{n!(n+\nu)!}y^{-n}\Big\{\ln(-y)+\psi(1+\nu+n)\\ +\psi(1+n)-\psi(B+n)-\psi(C-B-n)\Big\}+(-y)^{-A}\frac{\Gamma(C)}{\Gamma(B)}\sum_{n=0}^{\nu-1}\frac{\Gamma(\nu-n)(A)_n}{n!\Gamma(C-A-n)}y^{-n}\end{aligned}$$

where A, B and C are given in (3.15) and $\psi(z) = d\ln\Gamma(z)/dz$ is the digamma function. The second term with leading power y^{-A} corresponds to the non-normalizable piece, which vanishes when $\Gamma(B)$ has a pole, *i.e.* $-\frac{\omega}{2} + h_+ = -n$ is a non-negative integer. For this subset of frequencies, the analysis is more subtle since the first term might naively seem to vanish due to the $\Gamma(B)$ factor appearing in the denominator. However, notice that $\Psi(B+n)$ is also singular for this same subset of frequencies, and a careful limit gives the same result as before (3.20) for the normalizable modes.

3.3 Green functions from the method of images

The non-normalizable modes obtained in the previous section give the bulk to boundary propagator, Fourier transformed with respect to t and ϕ. We can also obtain the bulk to boundary propagator from a certain scaling limit of the bulk Feyman propagator on the orbifold. We can compute the Feynman Green function for scalar fields on the orbifold by the method of images: *i.e.* we start with the Feyman propagator in AdS_3 and then add all images under the orbifold action. This method implies a certain choice of vacuum on the orbifold that descends from the unique $SL(2,\mathbb{R})\times SL(2,\mathbb{R})$ invariant vacuum on AdS_3. The Feynman Green function on global AdS_3 [21] is

$$-iG_F(x,x') = \frac{1}{4\pi R}\left(z^2-1\right)^{-1/2}\left[z+\left(z^2-1\right)^{1/2}\right]^{1-2h_+}, \tag{3.33}$$

where $z = 1 + R^{-2}\sigma(x,\,x') + i\epsilon$, $\sigma(x,\,x')$ being the invariant distance among two points in the embedding space $\mathbb{R}^{2,2}$. That is, $\sigma(x,\,x') = \frac{1}{2}\eta_{MN}(x-x')^M(x-x')^N$ and for $\mu^2 > 0$

$$2h_+ = 1 + \sqrt{1+\mu^2}\,.$$

Thus, the Green function on the orbifold will be given by

$$-iG_{F/\Gamma}(x,x') = -i\sum_n G_F(x,x'_n) = \frac{1}{4\pi R}\sum_n \left(z_n^2-1\right)^{-1/2}\left[z_n+\left(z_n^2-1\right)^{1/2}\right]^{1-2h_+} \tag{3.34}$$

where we defined $z_n(x,x') = z(x,x'_n)$ and x'_n is the nth image point. It is easy to work out its value in the adapted coordinate system where the discrete identification is easy to implement. The answer is

$$z_n = \sin\Delta t\sinh\Delta\phi_n\sinh\tilde{\Delta}z + \cos\Delta t\cosh\Delta\phi_n\cosh\Delta z + i\epsilon\,,$$

where $\Delta t = t-t'$, $\Delta z = z-z'$, $\tilde{\Delta}z = z+z'$ and $\Delta\phi_n = \phi-\phi'+2\pi n$.

4. The holographic dual

Given an asymptotically AdS spacetime, the usual instruction concerning holography is that each disconnected component of the boundary will contain a copy of the canonical field theory dual of AdS space. These theories may be decoupled, entangled, interacting, identified or otherwise related depending on the specific circumstances. In the eternal BTZ black hole, for example, the two boundaries are thought to contain entangled copies of the D1-D5 CFT [3, 4]. By contrast, in AdS_2, which is a strip, there are subtleties concerning the status of the quantum mechanical dual

theories that could live on each boundary. It has been suggested that the theories on these two boundaries should be identified with each other [13, 14]. In explorations of holography in de Sitter space [7] similar issues have arisen: if there exists a field theory dual associated to the two de Sitter boundaries, should there be two entangled theories or should the two theories be identified?

In the present case, the spacetime (2.14), seen as an asymptotically AdS_3 spacetime, would appear to be dual to two (possibly entangled or interacting) copies of the D1-D5 CFT defined on the two null-cylinder boundaries. As we have seen, the surface at fixed radius on the orbifold is a boosted cylinder and the boost approaches infinity as the AdS boundary is reached, creating a null cylinder. This suggests the dual contains two DLCQ copies of the D1-D5 CFT. Another approach to duality might be to regard the dual as arising from an orbifold of the dual of AdS_3. Interestingly, as we have seen, the isometry under which we identify AdS is a conformal transformation of the boundary. This suggests that the dual is a "conformal orbifold" in which a theory is quotiented by a conformal transformation. We will compare and contrast these two approaches to the definition of a dual theory in Sec. 4.2.

Perhaps the most pedestrian way of approaching holography in AdS is to blindly apply the well-known prescription for computing correlation functions of a dual CFT on the boundary in terms of bulk data [16]. We have two related ways of approaching this – we can either use the bulk-boundary propagator prescription or the on-shell action prescription. Since this is the most concrete path towards duality, we will take it first in the section below.

4.1 Two point correlators and the choice of vacuum

The classic AdS/CFT correspondence [22] is defined by equating the partition function for string theory on AdS seen as a functional of boundary data to the generating function of correlation functions of the dual field theory [16]. In the semiclassical limit of the bulk theory (large N limit in the dual) this amounts to equating the bulk on-shell action to the boundary generating function of correlators. In our case there are two disconnected components to the boundary and the non-normalizable mode solutions whose boundary values are dual sources diverge on both boundaries. As we will see, this means that the on-shell action always has contributions from both boundaries. This suggests that the sources in the components of the dual theory on the two boundaries have correlated sources, but we will see that the situation is more subtle and interesting than the naive expectation, and that it is in fact possible to compute independent correlation functions within each boundary as well as between them.

Another approach to computing correlation functions of the dual to AdS space is to use a "bulk-boundary propagator" $G_{B\partial}$ in terms of which a diagrammatic expansion computes CFT correlators. We can define $G_{B\partial}$ by taking the boundary limit of the bulk Feynman propagator. From this perspective, it is possible to obtain a propagator from a single boundary into the bulk, in terms of which correlation functions of a dual defined on a single boundary or between boundaries can be obtained. We will compare these two approaches to correlation functions below.

Another tricky issue here is that in general, the basis of non-normalizable modes is ambiguous because one can add normalizable modes to the former without changing the growth near infinity.

In [4, 42] it was pointed out the choice of added normalizable modes has a bearing on the choice of vacuum for the AdS/CFT correspondence since the choice of non-normalizable modes in effect specifies the Fourier transform of the bulk-boundary propagator of the correspondence. It was also explained in [4, 42] that requiring the bulk-boundary propagator to arise from Euclidean continuation, namely as an analog to the bulk-bulk Feynman propagator, uniquely selected the normalizable component in the non-normalizable mode. Our spacetime does not have a Euclidean continuation. However, a distinguished basis of non-normalizable modes can be obtained by canceling the cut that appears in (3.29) as $y \to 0$ by addition of a normalizable mode (3.21). Below, we explore this issue which is related to the choice of vacuum for the orbifold.

4.1.1 Correlators from the method of images

First we make use of the expression (3.34) for the Feynman Green function on the orbifold $G_{F/\Gamma}$ to derive the bulk-boundary propagator. We use the notation $G_{B\partial\pm}$ for the propagator from the boundaries at $z \to \pm\infty$ to the bulk. To evaluate $G_{B\partial+}$ we send $z \to \infty$ in $G_{F/\Gamma}(x, x')$ (3.34) and rescale by $(e^{2h_+ z})$ to remove the standard asymptotic AdS falloff:

$$-iG_{B\partial+}(x, x') = \frac{1}{2\pi R} \sum_n \left(\cos \Delta t \cosh \Delta\phi_n e^{-z'} + \sin \Delta t \sinh \Delta\phi_n e^{z'} \right)^{-2h_+} , \tag{4.1}$$

where we omitted the $i\epsilon$ prescription. Similarly,

$$-iG_{B\partial-}(x, x') = \frac{1}{2\pi R} \sum_n \left(\cos \Delta t \cosh \Delta\phi_n e^{z'} - \sin \Delta t \sinh \Delta\phi_n e^{-z'} \right)^{-2h_+} . \tag{4.2}$$

Notice that both bulk-boundary propagators diverge as $z' \to \pm\infty$ when Δt or $\Delta\phi_n$ equals 0 (or indeed suitable multiples of π) but otherwise vanish in this limit. This confirms that these propagators diverge along the boundary lightcones as they should and vanish otherwise. (The additional singularities at integer multiples of π are explained below in terms of the periodicities of the bulk geodesics.)

We can use $G_{B\partial\pm}$ to compute correlation functions within the boundaries at $z \to \pm\infty$ and between them by taking the remaining bulk point to the appropriate boundary and rescaling again by $(e^{2h_+ z})$. We will only look at the correlator for nonzero Δt and $\Delta\phi_m$ since we are not interested in contact terms. Using $G_{\pm\pm}(\hat{x}, \hat{x}')$ to denote the possible two-point correlators, with $\hat{x}$, $\hat{x}'$ being points in the boundaries, we find:

$$-iG_{++}(\hat{x}, \hat{x}') = \frac{1}{2\pi R} (\sin \Delta t)^{-2h_+} \sum_n (\sinh \Delta\phi_n)^{-2h_+} , \tag{4.3}$$

$$-iG_{--}(\hat{x}, \hat{x}') = \frac{1}{2\pi R} (-1)^{-2h_+} (\sin \Delta t)^{-2h_+} \sum_n (\sinh \Delta\phi_n)^{-2h_+} , \tag{4.4}$$

$$-iG_{+-}(\hat{x}, \hat{x}') = -iG_{-+}(\hat{x}, \hat{x}') = \frac{1}{2\pi R} (\cos \Delta t)^{-2h_+} \sum_n (\cosh \Delta\phi_n)^{-2h_+} . \tag{4.5}$$

We can generate (4.5) from (4.3) by shifting $\Delta t \to \Delta t + \frac{\pi}{2}$ and $\Delta\phi_n \to \Delta\phi_n + i\pi/2$ (up to a constant phase). This agrees nicely with the fact that we can reach the second boundary from the first via

an excursion in the complex plane as described in Sec. 2.4. Notice that the G_{++} and G_{--} are singular when $\Delta t = 0$ or $\Delta\phi_n = 0$. This makes sense because ϕ and t are lightcone coordinates on the $z \to \pm\infty$ boundaries. By contrast G_{+-} is singular when $\Delta t = \pi/2$. This agrees with our analysis of geodesics: there is a null geodesic connecting points on opposite boundaries that are separated by $\Delta t = \pi/2$. Null geodesics can bounce from one boundary to the other and back again in time $\Delta t = n\pi$, accounting for the periodicity in the singularities of G_{++}. (Strictly speaking, for such integrally spaced intervals Δt the limiting procedure leading to (4.3) from (4.1) should be revisited since the second term with the parenthesis in (4.1) vanishes in these case.)

It is also instructive to calculate the correlation function in momentum space. The Fourier transform of G_{++} is:

$$\tilde{G}_{++}(\omega, m) = \int_{-\infty}^{\infty} dt \int_0^{2\pi} d\phi \; e^{i\omega t} e^{im\phi} G_{++}(t, \phi). \tag{4.6}$$

This is given by (we refer the reader to appendix A for details):

$$\tilde{G}_{++}(\omega, m) = \frac{i}{2\pi R}\,(-1)^{-2h_+}\frac{1}{4}\,\left(\frac{i}{2}\right)^{2h_+-1}\frac{1}{2^{2h_+}}\,(\Gamma(1-2h_+))^2\,\frac{\Gamma(h_+ - im/2)}{\Gamma(h_- - im/2)}\,\frac{\Gamma(-\omega/2+h_+)}{\Gamma(-\omega/2+h_-)}$$
$$\times\,\left(e^{i\theta} + (-1)^{-2h_+}\right)\left\{\frac{\sin(\pi(\omega/2+h_-))}{\sin(\pi(\omega/2+h_+))} + (-1)^{-2h_+}\right\}\,. \tag{4.7}$$

where

$$\frac{\csc\Big(\pi(h_+ + \frac{im}{2})\Big)}{\csc\Big(\pi(h_- + \frac{im}{2})\Big)} = e^{i\theta}\,. \tag{4.8}$$

This form of the correlation function will be useful for comparison with the on-shell action.

4.1.2 Correlation functions from boundary variation of the on-shell action

To compute dual CFT correlators from AdS action calculations we must choose a basis of non-normalizable modes. Since we can always add a normalizable piece to such a solution, the most general basis is

$$\bar{\Psi}(z,\, t,\, \phi) = e^{-i\omega\, t + i\, m\, \phi}\,\bar{\Psi}(z,\, \omega,\, m) = e^{-i\omega\, t + i\, m\, \phi}\,(\psi_{\text{non-norm}}(z,\, \omega,\, m) + C(\omega,\, m)\,\psi_{\text{norm}}(z,\, \omega,\, m))\,. \tag{4.9}$$

Since $\bar{\Psi}$ can be regarded as the Fourier transform of the bulk-boundary propagator, the frequency dependent coefficient $C(\omega, m)$ is related to the choice of vacuum implied by this basis. A distinguished basis of non-normalizable modes is determined by canceling the cuts in the solution as $y \to 0$ in (3.28) by the addition of a normalizable component. This requires that:

$$C(\omega,\, m) = -(-1)^{\nu}\frac{\Gamma(2h_-)\,\Gamma(-\frac{\omega}{2}+h_+)\,\Gamma(h_+ - i\frac{m}{2})}{\Gamma(2h_+)\,\Gamma(-\frac{\omega}{2}+h_-)\,\Gamma(h_- - i\frac{m}{2})} \equiv \mathcal{C}(\omega, m)\,. \tag{4.10}$$

The on-shell action is given by

$$S_{\text{bulk}} = \lim_{\Lambda\to\infty}\frac{1}{2}\cosh\,2\Lambda\Big(\int dt d\phi\,\bar{\Psi}\partial_z\bar{\Psi}|_{z=\Lambda} - \int dt d\phi\,\bar{\Psi}\partial_z\bar{\Psi}|_{z=-\Lambda}\Big)\,, \tag{4.11}$$

after integrating by parts and using the equations of motion in the metric (2.14). Writing

$$\bar{\Psi}(z,\, t,\, \phi) = \frac{1}{2\pi}\int d\omega \sum_m e^{-i\omega\, t + i\, m\, \phi}\, \bar{\Psi}(z,\, \omega,\, m)\ .$$

in momentum space, the on-shell action becomes

$$S_{\rm bulk} = \lim_{\Lambda\to\infty} \frac{\cosh 2\Lambda}{2}\int d\omega \sum_m (\bar{\Psi}(z,\omega,m)\partial_z \bar{\Psi}(z,-\omega,-m)|_{z=-\Lambda}^{z=\Lambda}\ . \tag{4.12}$$

It is convenient to rewrite this in terms of a bulk-boundary propagator $\mathcal{K}(z,m,\omega)$ which is normalized to approach 1 at the boundary. Since we have two boundaries here we must choose which one to normalize $\mathcal{K}$ on. Choosing $\mathcal{K}\to 1$ as $z\to\Lambda$ (where we take $\Lambda\to\infty$ at the end) we can write

$$\mathcal{K}_+(z,\, \omega,\, m) = \frac{\bar{\Psi}(z,\, \omega,\, m)}{\bar{\Psi}(\Lambda,\, \omega,\, m)}\ . \tag{4.13}$$

In terms of $\mathcal{K}_+$ a non-normalizable mode $\bar{\Psi}(z,\, t,\, \phi)$ whose Fourier components as $z\to\Lambda$ are $\bar{J}_+(\omega,\, m)$ can be written as

$$\bar{\Psi}(z,\, \omega,\, m) = \bar{J}_+(\omega,\, m)\, \mathcal{K}_+(\Lambda,\, \omega,\, m)\ . \tag{4.14}$$

Using this in the on-shell action (4.12) gives

$$S_{\rm bulk} = \lim_{\Lambda\to\infty} \frac{\cosh 2\Lambda}{2}\int d\omega \sum_m \bar{J}_+(\omega,\, m)\, \bar{J}_+(-\omega,\, -m)\, \mathcal{K}_+(z,\, \omega,\, m)\, \partial_z\, \mathcal{K}_+(z,\, -\omega,\, -m)|_{z=-\Lambda}^{z=\Lambda}\ . \tag{4.15}$$

The boundary two-point function evaluated in momentum space should then be

$$G'_{++}(\omega,m) = \frac{\delta S_{\rm bulk}}{\delta \bar{J}_+(\omega,\, m)\, \delta \bar{J}_+(\omega',\, m')}\ . \tag{4.16}$$

By construction we are considering the two-point function in the boundary at $z\to\infty$ since we specified the boundary data there; hence the notation G'_{++}. Note however that the boundary data at $z\to-\infty$ are fully specified also since

$$\mathcal{K}_+(-\Lambda,\, \omega,\, m) \to e^{-m\pi/2}\, e^{i\pi(\omega/2+h_-)} \quad \text{as} \quad \Lambda\to\infty\ . \tag{4.17}$$

Thus the two-point function picks up a contribution from both boundary terms (4.15) in the bulk action.

Computing the two-point function from (4.15) and (4.16) by explicitly using $\mathcal{K}_+$ is a tedious but straightforward exercise. We spare the reader the details, but recall that the basic philosophy, following [23] is to evaluate the action in a power series in e^Λ, drop singular contact terms, and extract the resulting contribution to the 2-point function. The leading term that contributes always arises from a interaction between the non-normalizable and the normalizable pieces of $\bar{\Psi}$ and hence of $\mathcal{K}$, and can readily be identified by the requirement of conformal invariance, which fixes the scaling with the cut-off Λ to be $\left(e^\Lambda\right)^{2-2\nu}$, where $\nu = h_+ - h_-$. Carrying out this computation

with $h_- < 0$ and $h_+ > 0$, and taking the functional derivatives, we obtain, after some suffering, a boundary 2-point function of the form.

$$G'_{++}(\omega, m) = \delta(\omega + \omega')\,\delta_{m+m'}\,\left(A_+\,C(\omega,\,m) + A_-\,C(-\omega,\,-m)\right)\ , \tag{4.18}$$

where the coefficients $A_\pm$ could depend on $\nu = h_+ - h_-$, m and ω. Both terms have contributions from both boundaries. Using (A.13) we can rewrite this as

$$G'_{++}(\omega, m) = C(\omega, m)\,Q'(\nu, \omega, m) \tag{4.19}$$

where Q' contains numerical coefficients and various trigonometric functions of the arguments. Note that, as described in Sec. 3.2.3, when ν is an integer the non-normalizable mode contains logarithms and so some further effort is necessary in the computations.

4.1.3 Comparison of the two methods

First of all consider the two-point function computed from the sum-on-images (4.7). Using

$$\frac{1}{\Gamma(2h_+)} = -\frac{1}{\pi}\Gamma(-\nu)\,\sin(\pi\,\nu) \quad ; \quad \Gamma(2h_-) = (-\nu)\,\Gamma(-\nu) \quad \Longrightarrow \quad \Gamma(-\nu)^2 = \frac{\Gamma(2h_-)}{\Gamma(2h_+)}\frac{\pi}{\nu\sin\pi\nu} \tag{4.20}$$

it is easy to show that the sum-on-images result is

$$\tilde{G}_{++}(\omega, m) = \mathcal{C}(\omega, m)\,Q(\nu, \omega, m) = -\frac{\Gamma(2h_-)\,\Gamma(-\frac{\omega}{2} + h_+)\,\Gamma(h_+ - i\frac{m}{2})}{\Gamma(2h_+)\,\Gamma - \frac{\omega}{2} + h_-)\,\Gamma(h_- - i\frac{m}{2})}\,(-1)^\nu Q(\nu, \omega, m) \tag{4.21}$$

where $\mathcal{C}$ is the special ratio of Gamma functions appearing in (4.10) and Q is a combination of numerical factors and trigonometric functions. This gives a result of the same form as the on-shell action computation (4.19) provided we pick a basis of non-normalizable modes in (4.9) with a normalizable component weighted by $C(\omega, m) = \mathcal{C}(\omega, m)$. As stated before, the choice of C amounts to a choice of vacuum, and setting $C = \mathcal{C}$ picks a vacuum in which possible cuts in the complex z plane for bulk-boundary propagator are absent. When $2h_+$ is an integer all the formulae are somewhat modified because of cancellations between factors that go to zero and to infinity in this limit, and because of the appearance of log terms in the non-normalizable modes. We do not investigate the details of this here since experience with the AdS/CFT correspondence has shown that correlation functions do not change qualitatively in the integer limit.

One boundary versus two: In the sum-on-images calculation it was clear that by taking different boundary limits of the bulk Feynman propagator we could calculate different boundary correlators, $G_{\pm\pm}$, between points on the same boundary and on opposite boundaries. The on-shell calculation initially appears to have a rather different character. As we discussed, the bulk non-normalizable modes diverge on both boundaries at the same time. A bulk-boundary propagator derived from them and normalized to 1 as $z \to \infty$ behaves as (4.17) as $z \to -\infty$. This suggests that sources for the dual CFT must be turned on in a correlated way in both boundary components. Transforming to position space, switching on a source $J_+(t,\,\phi)$ on the $z \to \infty$ boundary appears to switch on a source $J_-(t, \phi) = e^{i\pi\,h_-}\,J_+(t - \frac{\pi}{2},\,\phi + i\frac{\pi}{2})$ in the $z \to -\infty$ boundary. Thus, one of the

sources is turned on at a point that is shifted into the complex coordinate plane for the boundary theory. Sources at *real* coordinates appear to be independent of each other. Nevertheless, the correlation between sources on the two sides suggests that the dual need only consist of a theory on one of these boundaries. However, this is a misleading intuition as we learn by comparing with the BTZ black hole. The authors of [24, 5] compute the propagator from one of the two BTZ boundaries to a point in the bulk in the same asymptotic region and find:

$$K_{\rm BTZ}(r,u_+,u_-;u'_+,u'_-)=\sum_{n=-\infty}^{\infty}\frac{\left(\frac{r_+^2-r_-^2}{r^2}\right)^{h_+}\ e^{-2\pi h_+[T_+\,\Delta u_++T_-\,\Delta u_-+(T_++T_-)2\pi n]}}{\left\{\frac{r_+^2-r_-^2}{r^2}+(1-e^{-2\pi T_+[\Delta u_+2\pi n]})(1-e^{-2\pi T_-[\Delta u_-2\pi n]})\right\}^{2h_+}} \tag{4.22}$$

Here r is the radial coordinate of the BTZ black hole, $r_\pm$ are the coordinates of the outer and inner horizons, $u_\pm$ and $u'_\pm$ are lightcone coordinates in the bulk and boundary respectively, and $T_\pm$ are temperature parameters. As explained in [5] points can be transported from one asymptotic region of the eternal geometry to another by the transformations

$$T_\pm u_\pm \to T_\pm u_\pm \mp \frac{i}{2} \tag{4.23}$$

which are reminiscent of the discrete complex transformations in Sec. 2.4. Note that if $\Delta u_\pm = 0$, $K_{\rm BTZ}$ diverges as $r\to\infty$ as befits the Fourier transform of a non-normalizable mode in the BTZ spacetime. Applying the transformation (4.23) to the bulk point to move it to the other asymptotic region we find that the transformed propagator will diverge as $r\to\infty$ (thus approaching the second boundary) provided $\Delta u_\pm = \pm i/2$. Fourier transforming will thus lead to a non-normalizable mode that diverges at both boundaries. Alternatively if it is normalized to unity on one boundary it will pick up a momentum dependent phase at the other one. This is precisely the situation we have in our orbifold. Thus, just as in BTZ it is expected that we have independent sources and CFTs defined (at least at real coordinate points) on each conformal boundary.

We can follow this procedure from the BTZ black hole as follows. First, we have seen that the on-shell action, even expressed just in terms of J_+, collects contributions from both boundaries. If we expressed the action in terms of J_- we would get essentially the same result, agreeing with the fact that $G_{++}\sim G_{--}$ in the sum-on-images calculation. To compute G_{+-} from the bulk action, a natural prescription is to express one of the fields $\bar\Psi$ in the on-shell action (4.11,4.12) in terms of J_+ and the other in terms of J_-. In view of (4.17), it is easy to show that the resulting bulk action will lead to a two point function

$$G'_{+-}(\omega,m)\sim e^{-m\pi/2}e^{i\pi(\omega/2+h_-)}\,G'_{++}(\omega,m) \tag{4.24}$$

After Fourier transforming to position space we get

$$G'_{+-}(\Delta t,\Delta\phi)\sim G'_{++}(\Delta t-\pi/2,\Delta\phi+i\pi/2) \tag{4.25}$$

This exactly reproduces the shift relationship between the sum-on-images 2-point function G_{++} at $z\to\infty$ and G_{+-} between $z\to\pm\infty$. Thus both the on-shell action and sum-on-images approaches

are nominally capable of computing the correlators on either boundary or between them. The real question is whether these different pieces of data are independent or redundant information in a dual formulation. We will explore this further below.

4.2 Orbifold Holography

Above we approached holography on our orbifold by attempting to define on-shell action and bulk-boundary propagator approaches to computing CFT correlation functions. Here we explore general properties that the dual must have if (a) it is defined on the null boundary of our orbifold, or (b) it descends from the dual to global AdS_3 by our orbifold action.

4.2.1 Holography and DLCQ CFTs

A standard technique for computation in the AdS/CFT correspondence is to truncate the space at some fixed large radial coordinate which serves as a cutoff on the bulk. The field theory defined on the boundary surface is a regulated version of the CFT dual to the entire space, and sending the boundary to infinity corresponds to removing the cutoff. Let us imitate this procedure here.

The metric on fixed z surfaces is $g = l^2(-dt^2 + d\phi^2 + 2\sinh(2z)dt\, d\phi)$. As explained earlier, this is a boosted version of the usual timelike cylinder with the boost parameter approaching infinity as $|z| \to \infty$. Thus we expect that the dual theories theories living on each boundary are discrete light cone quantized (DLCQ) since they will have a compact null direction. The simplest way to work out the spectrum is to consider how the $U(1) \times SL(2,R)$ symmetries are realized on surfaces at fixed z. We can then work out the spectrum in the limits $z \to \pm\infty$ using representation theory.

As $z \to \infty$, the $SL(2,R)$ symmetry generators (3.3) and the $U(1)$ associated with ϕ become

$$\begin{aligned}
\bar{\mathcal{L}}_0 &= \frac{i}{2}\frac{\partial}{\partial\phi} \\
\mathcal{L}_0 &= \frac{i}{2}\frac{\partial}{\partial t} \\
\mathcal{L}_+ &= \frac{e^{2it}}{2}\left[\tanh(2z)\frac{\partial}{\partial t} + \frac{1}{\cosh(2z)}\frac{\partial}{\partial\phi} + i2h_+\right] \\
\mathcal{L}_- &= -\frac{e^{-i2t}}{2}\left[\tanh(2z)\frac{\partial}{\partial t} + \frac{1}{\cosh(2z)}\frac{\partial}{\partial\phi} - i2h_+\right],
\end{aligned} \tag{4.26}$$

The constant $2h_+$ appear when the generators acting on a representation with highest weight h_+. From the point of view of the bulk generators (3.3) this constant appears from the action of ∂_z on the asymptotic scaling of the normalizable modes. The latter three generators realize an approximate $SL(2,R)$ symmetry, up to terms of order e^{-4z} which are irrelevant in the large z limit. The fact that the $SL(2,R)$ only acts approximately at a fixed z is of course traced to the fact that cutting off the bulk imposes a cutoff in the dual CFT, breaking conformal invariance. If ϕ had not not been periodic as it is in our orbifold, there would have been a second approximate $SL(2,R)$ symmetry on surfaces of fixed z, generated by the first of the four operators above, and by two more obtained by exchanging t with $i\phi$ and ϕ with $-it$ in $\mathcal{L}_+$ and $\mathcal{L}_-$. However, the resulting exponential dependence on ϕ leads to generators that are not well-defined on the orbifold since $\phi \sim \phi + 2\pi$. Thus the second

possible $SL(2,R)$ does not exist even in an approximate sense at any fixed z. So as $z \to \infty$ the symmetry generators of the dual as inherited from the bulk are:

$$\begin{aligned}
\bar{\mathcal{L}}_0 &= \frac{i}{2}\frac{\partial}{\partial\phi} \\
\mathcal{L}_0 &= \frac{i}{2}\frac{\partial}{\partial t} \\
\mathcal{L}_+ &= \frac{e^{2it}}{2}\left[\frac{\partial}{\partial t} + i2h_+\right] \\
\mathcal{L}_- &= -\frac{e^{-2it}}{2}\left[\frac{\partial}{\partial t} - i2h_+\right]
\end{aligned} \tag{4.27}$$

The latter three operators exactly generate the $SL(2,R)$ algebra $[\mathcal{L}_0, \mathcal{L}_\pm] = \mp\mathcal{L}_\pm$ and $[\mathcal{L}_+, \mathcal{L}_-] = 2\mathcal{L}_0$. By simply examining the metric $ds^2 \propto dt\, d\phi$ on the $z \to \infty$ surface it my seem surprising that two $SL(2,R)$s are not present as boundary reparameterizations of t and ϕ, but this is because of the limiting procedure described above. A similar analysis applies as $z \to -\infty$.

The spectrum of the dual theory at $z \to \infty$ will carry charges (ω, m) under $\mathcal{L}_0$ and $\bar{\mathcal{L}}_0$. Since ϕ is periodic, m will be an integer and the corresponding wavefunction will have a factor $e^{im\phi}$. A highest representation of the $SL(2,R)$ is given by $\mathcal{L}_-|0\rangle = 0$, $|n\rangle = \mathcal{L}_+^n|0\rangle$, such states will be eigenfunctions of $\mathcal{L}_0$ with eigenvalue $\omega/2 = h_+ + n$ with n a non-negative integer. The corresponding wavefunction will have a factor $e^{-i(2h_+ + 2n)t}$. The same analysis applies at $z \to -\infty$.

Actually as $z \to \infty$ only negative m are allowed for reasons of unitarity. This is expected from the DLCQ perspective, but the easiest way to see it here is to observe that both ϕ and t are null directions. Since the metric is $ds^2 \propto dt\, d\phi$, if we consider states with positive $P_t \sim$ Energy then for non-tachyonic excitations (i.e. positive effective mass squared) it must follow that $P_t\, P_\phi \leq 0$. Since $P_t = 2\mathcal{L}_0 > 0$, it follows that $P_\phi = 2\bar{\mathcal{L}}_0 \leq 0$. With our conventions that the wavefunction is proportional to $e^{im\phi}$, this implies that $m \geq 0$ for the theory on the $z \to \infty$ boundary. On the $z \to -\infty$ boundary, the metric becomes $ds^2 \propto -dt\, d\phi$ and so we will similarly conclude that $m \leq 0$.

Overall the spectrum exactly matches the results from the bulk – states carry integer $U(1)$ charges and realize a complete $SL(2,R)$. The novelty, that can be traced to the infinite boost at each boundary, is that the positive (negative) m eigenvalues are realized on different boundaries. This nicely meshes with the localization of positive (negative) m normalizable modes in the $z > 0$ ($z < 0$) regions of the bulk.

4.2.2 Conformal orbifolds of CFTs

Since our spacetime is an orbifold of global AdS_3 we can try to orbifold its CFT dual to construct the field theory describing our spacetime. Recall again that AdS_3 has an $SL(2,R)_L \times SL(2,R)_R$ isometry group that is the same as the conformal group of the dual 2d CFT. We chose a basis of generators $\xi_i^\pm$ for this isometry group in eqs. (2.4) and (2.6). Explicit expressions for these generators in terms of the global AdS_3 coordinates (2.3) are easily obtained by comparing our isometry generators with those defined in [15] (see Sec. 4, especially Sec. 4.3 of that paper). We

find that

$$\xi_1^+ \equiv -L_1 = -\partial_w \tag{4.28}$$

$$\xi_2^+ \equiv L_3 = = \left(\frac{\cosh 2\rho}{\sinh 2\rho}\right)\cos w\,\partial_w - \frac{\cos w}{\sinh 2\rho}\partial_{\bar{w}} + \frac{\sin w}{2}\partial_\rho \tag{4.29}$$

$$\xi_3^+ \equiv -L_2 = \left(\frac{\cosh 2\rho}{\sinh 2\rho}\right)\sin w\,\partial_w - \frac{\sin w}{\sinh 2\rho}\partial_{\bar{w}} - \frac{\cos w}{2}\partial_\rho \tag{4.30}$$

where $w = \tau + \theta$ and $\bar{w} = \tau - \theta$ in terms of global coordinates (2.3). These generators satisfy the $\mathrm{SL}(2,\mathbb{R})$ commutation relations $[L_1, L_2] = -L_3$, $[L_1, L_3] = L_2, [L_2, L_3] = L_1$. The expressions for ξ^- are obtained similarly. Notice that as we approach the AdS_3 boundary $\rho \to \infty$ the generators on a fixed ρ surface become

$$\xi_1^+ \to -\partial_w \quad ; \quad \xi_2^+ \to \cos w\,\partial_w \quad ; \quad \xi_3^+ \to -\sin w\,\partial_w \tag{4.31}$$

which are the standard left-moving $SL(2,R)$ generators of the cylinder. (The ξ^- give rise to the right-moving $\mathrm{SL}(2,\mathbb{R})$.) The orbifold studied in this paper is an identification of AdS_3 by the action of ξ_2^+, which is a conformal transformation $\cos w\,\partial_w$ of the boundary.

Orbifolds by a conformal transformation are not very familiar, so it is helpful to study an example: the free boson on the cylinder. In order to orbifold by the conformal transformation $\cos w\,\partial_w$ we should study states satisfying:

$$e^{i2\pi\cos w\,\partial_w}\,|s\rangle = |s\rangle \tag{4.32}$$

or equivalently

$$\cos w\,\partial_w\,|s\rangle = k\,|s\rangle \quad ; \quad k \in Z \tag{4.33}$$

The wavefunction for the free boson can be split into left and right moving pieces $|s\rangle = f(\bar{w}) + g(w)$. While $f(\bar{w})$ can be any suitable right moving wavefunction,

$$\frac{\partial g}{\partial w} = \frac{kg}{\cos w} \quad \Longrightarrow \quad g(w) = A\left[\frac{1+\sin w}{\cos w}\right]^k \tag{4.34}$$

For $k = 0$ the left-moving wavefunction $g(w)$ is constant. When $k > 0$ ($k < 0$), $g(w)$ is singular at $w = \pi/2$ ($w = -\pi/2$).[6] The integer parameter k appearing here should be identified with the integer $U(1)$ charge carried by solutions to the wave equation on the orbifold spacetime since in both cases we are considering eigenstates of $\xi_2^+ \equiv L_3$. In the DLCQ picture for the dual to the orbifold, the states of positive and negative k appear to be represented separately on the left and right boundary DLCQ theories each of which represents one tower of positive left or right moving momenta. These sets of momenta, taken together, should be associated with quantum number k appearing above in the conformal orbifold picture of the dual CFT. The $SL(2,R)$ arising from the right-movers of the conformal orbifold picture is realized in the DLCQ picture by the $SL(2,R)$ that will act separately on the tower of right or left moving momentum states that survive the DLCQ limit in each boundary.

[6] For $k > 0$ $g(w)$ is singular when the denominator vanishes at $w = \pi/2$. Both the numerator and the denominator vanish at $w = -\pi/2$, but in this case L'Hôpital's rule shows that $g(w) \to 0$ as $w \to -\pi/2$. Similarly the singularity is at $w = -\pi/2$ for $k < 0$.

One CFT or two: Entangled states and interactions The interesting picture that emerges from the discussion above is that the dual to our orbifold spacetime can be equivalently thought of as a "conformal orbifold" of a CFT on a cylinder, or a sum of two DLCQ theories. The latter theories are separated by the bulk spacetime and the positive and negative $U(1)$ charges of the conformal orbifold appear separately as right/left moving momenta surviving the two DLCQ limits. (There is some subtlety concerning the states with zero $U(1)$ charge.) All of this strongly suggests that in the DLCQ picture both boundaries are necessary to construct a complete dual, as in the eternal BTZ black hole, and unlike some suggestions made in AdS_2 and in de Sitter space.

A key question is what is the vacuum state for this proposed dual? In the case of BTZ black holes choosing the Hartle-Hawking vacuum for the bulk spacetime leads to a particular entangled state in the two dual CFTs [3, 4]. We cannot follow a parallel logic here because of the absence of a Euclidean continuation. Nevertheless, as we will see in Sec. 5.1, our orbifold can be obtained as a Penrose-like focussing limit of the BTZ black hole. The corresponding limit of the BTZ dual will lead to an entangled state in two components of the dual to our spacetime. The discrete excursions in the complex coordinate plane that transport points in one boundary to the other and back again (Sec. 2.4, and the resulting complex transformations relating correlation functions on a single boundary (4.3) and between boundaries (4.5), lead to a similar conclusion). Indeed, one can easily write down an entangled state between the two boundary theories that reproduces the required symmetries and relations between 2-point correlators (4.3) and (4.5). However, compared to BTZ, the additional challenge here is that the two boundaries are causally connected through the bulk and thus we expect interactions between the two dual components. In particular, because there are no global horizons in our orbifold, the Hilbert space does not naturally separate into a product with decoupled Hamiltonians acting on each part, although the localization of $m > 0$ ($m < 0$) modes at $z > 0$ ($z < 0$) is suggestive. We are investigating how the appropriate vacuum and interactions can be understood from the dual perspective.

5. String duality and holography

In Sec. 2 we have seen that the spacetime (2.14) arises from at least two different perspectives: (i) as non-singular, causally regular discrete quotients of global AdS_3 whose generator is a very particular combination of boosts, and (ii) as an S^1 fibration over AdS_2. In this section, we will discuss a third inequivalent way of getting our orbifold spacetime: as a Penrose-like limit focusing on the vicinity of the horizon of extremal BTZ black holes. We will also embed these constructions in string theory, and by using U-duality and liftings to M-theory, we will generate several dual descriptions to our original spacetime in type IIA, IIB and M-theory. Matrix models emerge as the holographic dual in several of these dual perspectives, perhaps providing some link with the well-known appearance of matrix models as a dual description of 2d gravity [26].

5.1 Penrose-like limits of the D1-D5 string and holography

In type IIB string theory on T^4, the near horizon limit of Q_1 D1 branes sharing a non-compact direction with Q_5 D5 branes wrapped on the T^4 is $AdS_3 \times S^3 \times T^4$. If we compactify the common

spatial direction shared by the two sets of branes on a circle of radius R, and put n units of left or right moving momentum on this circle, the spacetime becomes an extremal 5d black hole whose near-horizon limit is the extremal (mass = angular momentum), rotating BTZ black hole times $S^3 \times T^4$. As shown by Strominger and collaborators [12, 13, 14], the discrete quotient we have considered in this paper arises universally as a Penrose-like "very-near-horizon" limit of this black hole.

In terms of the 5d black hole charges (Q_1, Q_5, n) the near-horizon BTZ metric is

$$g = l^2 T^2 \left(dx + \frac{dt}{R} \right)^2 + \frac{U^2}{l^2} \left((R\, dx)^2 - dt^2 \right) + l^2 \frac{dU^2}{U^2} \,. \tag{5.1}$$

where $\frac{n}{R}$ is the momentum along the compact direction of the D1-D5 system, l is the AdS scale, $T^2 = n/(Q_1 \cdot Q_5)$, and x is identified as $x \sim x + 2\pi$. It is useful to introduce a new radial coordinate

$$r^2 = \frac{U^2 \cdot R^2}{l^2} + l^2 \cdot T^2 \ , \quad r \in [l\, T,\, \infty) \ . \tag{5.2}$$

The metric (5.1) in the new coordinate (5.2) acquires the standard BTZ form, after a rescaling of the timelike coordinate, $t \to R\,\tau/l$:

$$g = -\frac{(r^2 - l^2 T^2)^2}{r^2\, l^2}\, d\tau^2 + \frac{r^2\, l^2}{(r^2 - l^2 T^2)^2}\, dr^2 + r^2 \left(dx + \frac{l\, T^2}{r^2}\, d\tau \right)^2 \ . \tag{5.3}$$

In these coordinates, it is clear that the black hole has a horizon at $r_+ = l \cdot T$.

The "very-near-horizon" limit introduced in [13], and also used in [14],

$$\frac{U^2 \cdot R^2}{l^4 \cdot T^2} \to 0 \ , \tag{5.4}$$

is a focusing limit in the geometry close to the horizon of the extremal black hole, $r \to r_+$, as is easily checked by taking this limit in (5.2). We can think about this limit in various ways: $U \to 0$ with R and T, $R \to 0$ with U and T fixed, $n \to \infty$ where n is the momentum along the D1-D5 string with all other quantities fixed, etc. In whichever way we choose to think, this is a Penrose-like limit in the sense that we are focusing on a null surface. Of course, an actual Penrose limit focuses on a null *geodesic*. However, we will see some further analogies between these two kinds of limits.

The BTZ geometry described by (5.3) is locally AdS_3, and is obtained by discrete identifications of AdS_3. In the Poincaré patch description of AdS_3

$$ds^2 = \frac{l^2}{y^2} \left(d\omega^+\, d\omega^- + dy^2 \right) \ ,$$

the identification $x \sim x + 2\pi$ in (5.1) corresponds to [13]

$$\begin{aligned} \omega^+ &\sim e^{4\pi T}\, \omega^+ \ , \\ \omega^- &\sim \omega^- + 2\pi R \ , \\ y &\sim e^{2\pi T}\, y \,. \end{aligned} \tag{5.5}$$

This identification is generated by the following Killing vector:

$$\xi = 2\pi \left(R\, \partial_{\omega^-} + T \left(2\omega^+ \partial_{\omega^+} + y \partial_y \right) \right) .$$

In terms of the generators (see (2.4)) of $\mathrm{SO}(2,2)$ acting linearly in $\mathbb{R}^{2,2}$ in which AdS_3 is embedded, this Killing vector is

$$\xi = 2\pi R \left(J_{02} - J_{01} + J_{13} - J_{23} \right) + 2\pi T \left(J_{12} - J_{03} \right) . \tag{5.6}$$

As explained in [13], in the "very-near-horizon" Penrose-like limit, the geometry is obtained by keeping only the latter term in the generator (5.6) of the identification. Thus it corresponds to $R \to 0$ or $T \to \infty$ (which implies $n \to \infty$ since we are are keeping Q_1 and Q_5 fixed in order to fix the AdS scale and the torus moduli) combined with rescalings to normalize the generator. In this limit, we recover the self-dual identification that we have been discussing in this paper since the dominant second term in the generator (5.6) is related to (2.7) by a rotation in the $\{x^2 , x^3\}$ plane by $\pi/2$, which is an isometry.

This Penrose-like limit strongly suggests that the dual to our orbifold involves the DLCQ of the D1-D5 string. The momentum along this string is n/R. Therefore, sending $R \to 0$ or $n \to \infty$ as required by the very-near-horizon limit is equivalent to studying the physics in the infinite momentum frame of the D1-D5 string, leading to a DLCQ-like description [7] Interestingly, the $R \to 0$ limit achieves this even if the number of quanta of momenta, namely n, is fixed. Since the fixed n geometries realize all the extremal 5d black holes in this compactification, and equivalently all the extremal BTZ geometries [27], we are studying the properties of the vicinity of the horizon of these black holes. We learn the geometry in this region is universal, as is its dual description as a DLCQ theory. It is interesting that the extremal 5d black holes appearing here are precisely the ones whose states have been counted in string theory [28]. There is even a limit in which the 4d extremal black holes of string theory whose states can be counted [29] display a BTZ in the near-horizon [30]. Thus we are in a sense studying the universal properties of the horizon of all black holes whose entropy is understood fully in string theory.

An interesting analogy between this emergence of our orbifold from a focus on a null surface, and the emergence of a pp-wave from the focus on a null geodesic [32, 33], is that both spacetimes have a null boundary [34]. In our case the boundary is a null cylinder while the pp-wave has a null line boundary. In the next section we will see that from one perspective the dual to our orbifold is related to a quantum mechanical theory, just as the pp-wave should be. A productive methodology in the pp-wave case was to implement the Penrose limit as an operation in the dual to the full AdS spacetime, thereby isolating the sector of the full CFT that is needed to describe the pp-wave [35]. A useful approach here might be to consider an analogous operation focusing on a sector of the dual to the BTZ black hole which has also been extensively studied.

[7] The infinite momentum frame also arose in the context of AdS/CFT for waves propagating in the worldvolume of M2, D3 and M5-branes, by taking the Maldacena decoupling limit keeping the momentum density of the wave fixed [31] .

On the origin of symmetries: The first thing to understand is how the $U(1) \times U(1)$ isometry group of the BTZ black hole (generated by the vector fields ∂_t and ∂_x) goes over to the $U(1) \times SL(2,R)$ isometry group of the Penrose-like limit, namely our orbifold. In terms of the Poincaré generators

$$\begin{aligned} \partial_t &= \frac{T}{R}\left(2\omega^+\partial_{\omega^+} + y\partial_y\right) - \partial_{\omega^-} \\ \partial_x &= 2\pi\left(R\partial_{\omega^-} + T\left(2\omega^+\partial_{\omega^+} + y\partial_y\right)\right) \ . \end{aligned} \tag{5.7}$$

After the rescaling $t \to \frac{R}{l}\tau$ the natural "Hamiltonian" in BTZ coordinates is

$$\partial_\tau = \alpha\left(\frac{T}{l}\left(2\omega^+\partial_{\omega^+} + y\partial_y\right) - \frac{R}{l}\partial_{\omega^-}\right) \ . \tag{5.8}$$

Thus, in the Penrose-like limit in which $R \to 0$ or $T \to \infty$, ∂_τ and ∂_x coincide and give identical quantum numbers. This $U(1)$ which survives the limit is the compact $U(1)$ generator of our orbifold. The $SL(2,R)$ that emerges is a new enhanced symmetry appearing in the limit. This is reminiscent of the enhanced symmetries that can appear in the Penrose limits of AdS space [33, 36].

On entangled states: Eternal non-extremal BTZ black holes have a dual description in terms of two copies of the D1-D5 CFT in an entangled state [3, 4, 5]. Following the conventions of [5] the temperature T and angular momentum potential Ω of the non-extremal BTZ can be combined into

$$\frac{1}{T_\pm} \equiv \frac{1}{T} \pm \frac{\Omega}{T}$$

where $T_\pm$ are related to $r_\pm$ by

$$r_\pm = \pi l(T_- \pm T_+)$$

The non-extremal BTZ is then dual to two decoupled conformal field theories living in an entangled state

$$|\Psi> = \sum_{E,J} e^{-\beta_H(E-\Omega J)} |E,J>_1 \, |E,J>_2 \ , \tag{5.9}$$

where, effectively, we can described the Penrose-like limit by $\Omega \to 1$ and $\beta_H \to \infty$ in the entangled state.[8] The precise state that results then depends on how E approaches J as β diverges. As we have already described a DLCQ limit is also involved since an infinite momentum limit is effectively being taken at the same time. We will not explore this structure any further here, but the appearance of two entangled theories from the Penrose-like limit justifies again our assertion that that our orbifold is related to an entangled state in two theories.

5.2 Compactification, two dimensional gravity and quantum mechanics

As mentioned in section 2.1, our spacetime (2.14) contains a circle of constant radius. The direction along the circle is a direction of isometry. Thus we can compactify on this circle getting a two-dimensional effective description. The latter is more easily obtained from the explicit S^1 fibration

[8] The maximally extended non-extremal BTZ actually has many asymptotic regions if we include the region beyond the singularity. See [5] for a very interesting discussion of entanglement between dual theories living on all of the asymptotic components.

over AdS_2 given in (2.19), giving rise to

$$\begin{aligned} g_2 &= -\cosh^2 2z\, dt^2 + dz^2 \ , \\ A_1 &= \sinh 2z\, dt \end{aligned} \tag{5.10}$$

where A_1 stands for an electric arising from the off-diagonal component of the 3d metric (2.14) and g_2 is exactly the AdS_2 metric. Thus our spacetime is equally well described as AdS_2 deformed by the addition of a constant electric field. (See [13] for an earlier discussion of these points.) Scalar field modes carrying momentum in the ϕ direction of our orbifold will carry electric charge on AdS_2 after compactification. Because of the background electric field, positive (negative) charges will be attracted towards the $z \to \infty$ ($z \to -\infty$) boundary. This nicely matches the localization of bulk wavefunctions with angular momentum on the orbifold, and also with the splitting of $m > 0$ and $m < 0$ states into the two boundary CFTs. The boundary of AdS_2 consists of two real lines and thus the dual, from this perspective, should be a $0+1$d quantum mechanical theory. There has been discussion in the literature concerning whether or not the dual lives on both boundary components. Above we saw evidence that both boundaries are needed to describe our spacetime. Anyway, the dual in our case cannot be simply the dual to AdS_2 because the electric field implies a deformation of the latter. Following the discussion in the previous section about the emergence of our spacetime from the D1-D5 string we can conclude that the dual quantum mechanics emerges after rescaling a very low energy limit of the dynamics of this string in a sector of fixed but very large angular momentum. The appearance of 2d gravity could be a signal of instabilities in our model since back reaction effects are usually very large in 2d, leading for example to fragmentation effects which necessitate a sum over geometries [14]. However, if we regard our space as the effective description of the vicinity of the black hole horizon in an asymptotically flat spacetime or of the BTZ horizon, then this issue can be disregarded. The connection with 2d gravity suggests the possibility that a Matrix model is somehow involved and the appearance of a DLCQ from the 3d perspective gives similar indications.

5.3 Dual backgrounds

The orbifold of AdS_3 we are considering has a compact direction. Thus when embedded in string theory, it is natural to study T-duality transformations along it and/or the lift to M-theory of this background.

We will start with the $AdS_3 \times S^3 \times \mathbb{T}^4$ that is obtained as the near horizon limit of a system of D1 and D5-branes. We will follow the conventions defined in [37]. Thus all coordinates are dimensionless, the length units begin carried by the components of the metric. The fluxes are also dimensionless, which means that these fields have been normalized in such a way that there are different powers of α' in the effective supergravity action.

We start with the near horizon limit of the D1-D5 system [38]

$$\begin{aligned} g &= l^2\,(g_{\mathrm{AdS}_3}+g_{\mathrm{S}^3})+\alpha'\sqrt{\frac{Q_1}{v\,Q_5}}dx^i\,dx_i\ , \\ F_3 &= d\,C_2 = Q_5\left(\mathrm{dvol}\,\mathrm{S}^3+\star_6\mathrm{dvol}\,\mathrm{AdS}_3\right)\ , \\ e^{-2\Phi} &= \frac{v\,Q_5}{g_s^2\,Q_1}\,, \end{aligned} \tag{5.11}$$

where $l^2 = g_s\,\alpha'\sqrt{Q_1\cdot Q_5/v}$. Q_1 and Q_5 stand for the charges of the original D1 and D5-branes, whereas v determines the volume of the 4-torus. In particular, we are considering a square torus in which $x^i \sim x^i + 2\pi(\alpha')^{1/2}v^{1/4}$ $i=1,2,3,4$. To describe the self-dual orbifold, we just replace g_{AdS_3} by the metric appearing in (2.14) setting $l=1$. The RR flux, in adapted coordinates (2.13) is

$$F_3 = Q_5\left(\mathrm{dvol}\,\mathrm{S}^3+\beta\cosh 2z\,dt\wedge d\phi\wedge dz\right)\ . \tag{5.12}$$

In particular, its potential C_2 has non-trivial components $C_{t\phi}=\beta\,Q_5\sinh 2z$[9].

For this classical solution to be reliable, the string coupling constant should be small. Also, for small α' corrections, we require that the radius be bigger than the string scale, otherwise we should use the T-dual description. These two conditions are summarized below

$$\frac{v\,Q_5}{g_s^2\,Q_1} > 1 \quad \text{(weak coupling)} \tag{5.13}$$

$$g_s\left(\frac{Q_1\,Q_5}{v}\right)^{1/2} > 1 \quad (R^2_{\text{eff}}>\alpha')\ . \tag{5.14}$$

Let us explore the different descriptions of our spacetime as we vary the coupling and the effective radius of the compact dimension.

S-duality: At strong coupling, the S-dual configuration is more reliable. After the S-duality transformation, the string coupling constant will just be inverted ($\Phi\to-\Phi$), the RR two-form is interchanged with the NS-NS two-form potential (B_2) (with a minus sign) and the metric in the string frame is just obtained from requiring the metric on the Einstein frame to be invariant under the transformation. The final S-dual configuration is summarized below :

$$\begin{aligned} g &= \alpha'\,Q_5\,(g_{\mathrm{AdS}_3}+g_{\mathrm{S}^3})+\frac{\alpha'}{g_s}dx^i\,dx_i\ , \\ H_3 &= -\alpha'\,Q_5\left(\mathrm{dvol}\,\mathrm{S}^3+\star_6\mathrm{dvol}\,\mathrm{AdS}_3\right)\ , \\ e^{-2\Phi} &= \frac{g_s^2\,Q_1}{v\,Q_5}\,. \end{aligned} \tag{5.15}$$

The range of validity of this description is again constrained by two conditions

$$\begin{aligned} \frac{v}{Q_1\,Q_5} &< \left(\frac{g_s}{Q_5}\right)^2 \quad \text{(weak coupling)} \\ \beta^2\,Q_5 &> 1 \quad (R^2_{\text{eff}}>\alpha')\ . \end{aligned} \tag{5.16}$$

[9]The orbifold discussed in Sec. 2 corresponds to $\beta=1$. It is straightforward to introduce a free parameter, corresponding to the rapidity of the boosts defining the orbifold action by rescaling the coordinate ϕ.

S-duality followed by T-duality: If the radius of the compact direction becomes much smaller than the string scale in (5.15), we need to go to a T-dual description of the above S-dual configuration. As already noticed in [11], the self-dual orbifold of AdS_3 has the significant property that if we apply the T-duality transformations [39] along the fiber generated by ∂_ϕ, the type IIA configuration thus obtained has the same geometry. Technically, this property can be easily seen by the fact that the metric cross term $g_{t\phi}$ and the NS-NS 2-form potential component, $B_{t\phi} = -\beta\, Q_5 \sinh 2z$ are identical. So under their exchange (T-duality), the geometry will not be modified. There is effectively just a rescaling of the original β parameter, due to the transformation of the radius of the compact direction under T-duality. In other words, the T-dual geometry is given in terms of (5.15) but with a new parameter $\beta' = (\beta\, Q_5)^{-1}$. This description is good when both conditions (5.16) are violated. Notice that the self-dual radius is given by $\beta^2 = (Q_5)^{-1}$.

T-duality: We now consider the T-dual configuration of (5.11). This is natural when the effective radius of the compact direction ϕ becomes smaller than the string scale. The T-dual configuration is

$$\begin{aligned}
g &= l^2\,(g_{\mathrm{AdS}_2} + g_{\mathrm{S}^3}) + \alpha'\,\frac{1}{g_s}\sqrt{\frac{v}{Q_1\,Q_5}}\,d\phi^2 + \alpha'\sqrt{\frac{Q_1}{v\,Q_5}}dx^i\,dx_i\ , \\
d\,C_3 &= Q_5\,\big(\mathrm{dvol}\,\mathrm{S}^3\wedge d\phi\big)\ , \\
C_1 &= \beta\,Q_5\,\sinh 2z\,dt\ , \\
B_2 &= -\frac{1}{2\beta}\sinh 2z\,dt\wedge d\phi\ , \\
e^{-2\Phi} &= \frac{(\beta\,Q_5)^2}{g_s}\sqrt{\frac{v}{Q_1\,Q_5}}\,.
\end{aligned} \tag{5.17}$$

The geometry is given by $AdS_2 \times S^3 \times S^1 \times \mathbb{T}^4$. The conformal boundary of this metric is the conformal boundary of AdS_2, that is, two real lines.

T-duality followed by M-theory lift: The above T-dual description is reliable at weak coupling,

$$\frac{(\beta\,Q_5)^2}{g_s}\sqrt{\frac{v}{Q_1\,Q_5}} > 1\ .$$

However at strong string coupling, an eleventh dimension y opens up, giving rise to the eleven dimensional configuration:

$$\begin{aligned}
\frac{g}{l_p^2} &= \left((g_s\,\beta\,Q_5)^2\,\frac{Q_1\,Q_5}{v}\right)^{1/3}\big(-\cosh^2 2z\,dt^2 + dz^2 + g_{\mathrm{S}^3}\big) + \left(\frac{\beta\,v}{g_s^2\,Q_1}\right)^{2/3}\,d\phi^2 \\
&\quad + \left(\frac{\beta^2\,Q_1}{v\,g_s}\right)^{1/3}\,dx^i dx_i + \left(g_s^2\,\frac{Q_1\,Q_5}{v}\,(\beta\,Q_5)^{-4}\right)\,(dy + \beta\,Q_5\,\sinh 2z\,dt)^2 \\
F_4 &= dC_3 - dy\wedge H_3 = \big(Q_5\,\mathrm{dvol}\,\mathrm{S}^3 - \beta^{-1}\mathrm{dvol}\,\mathrm{AdS}_2\wedge dy\big)\wedge d\phi
\end{aligned} \tag{5.18}$$

This, again has the topology of an S^1 fibration over AdS_2 times $S^2 \times S^1 \times \mathbb{T}^4$.

5.4 Asymptotically flat construction

It is interesting to study the asymptotically flat counterparts of the various asymptotically AdS solutions given in Sec 5.3. Our main motivation is that in the aymptotically flat constructions, these spacetimes acquire a brane interpretation, which can provide some intuition concerning the dynamics of the system. We start with the D1-D5 system with momentum along the common direction, which leads to an $AdS_3 \times S^3$ factor in the near horizon limit. In the asymptotically flat spacetime, the momentum is described by adding a third conserved charge, which leads us to add a third harmonic function which would source this charge. Our discussion is analogous to that for the non-dilatonic branes in [31]. We follow the same strategy but for the non-dilatonic D1-D5 system. Therefore, we consider the metric ansatz

$$\frac{g}{\alpha'} = (f_1 \cdot f_5)^{-1/2} \left\{(W-2)dt^2 + W\, dz^2 - 2(W-1)\, dt\, dz\right\} + f_1^{1/2}\, f_5^{-1/2}\, dx^i dx_i \\ + (f_1 \cdot f_5)^{1/2} \left(dr^2 + r^2\, g_{S^3}\right) , \quad (5.19)$$

where

$$f_1 = 1 + \frac{\alpha'\, g_s\, Q_1}{v\, r^2} \quad , \quad f_5 = 1 + \frac{\alpha'\, g_s\, Q_5}{r^2} \quad , \quad W = 1 + \frac{\alpha'\, N}{v\, r^2} ,$$

and N could still depend on the string coupling constant g_s. Here, z is an angular variable. The solution of type IIB equations of motion requires non-trivial dilaton and RR three-form field strength. These are given by

$$e^{2\Phi} = g_s^2\, \frac{f_1}{f_5} , \\ F_3 = -g_s^{-1}\, df_1^{-1} \wedge dt \wedge dz + 2Q_5 \mathrm{dvol}\, S^3 . \quad (5.20)$$

The near horizon limit of such pp-waves propagating in non-dilatonic branes does not lead to the AdS space. Instead, we obtain the Kaigorodov spacetime (see [31] for details). Interestingly, in three dimensions, Kaigorodov spacetime is known to be equivalent to the extremal BTZ black hole. Therefore, taking the standard decoupling limit, keeping the momentum density of the wave fixed, we get the construction in (5.1), which was discussed in [13]. Then, after a very-near-horizon limit (5.4) leads to a local description of the orbifold of AdS_3 under discussion in this paper.

As is Sec 5.3 it is interesting to perform duality transformations on this solution.

S-duality: We now consider the S-dual of the configuration in (5.19) and (5.20). Given the brane interpretation of this type IIB configuration, it is clear that the S-dual configuration will be a F1-NS5 system with some momentum (wave) propagating along the common direction. Indeed, the metric, dilaton and fluxes in the S-dual are given by:

$$e^{2\Phi} = g_s^{-2}\, \frac{f_5}{f_1} , \\ H_3 = g_s^{-1}\, df_1^{-1} \wedge dt \wedge dz - 2Q_5 \mathrm{dvol}\, S^3 , \quad (5.21) \\ \frac{g}{\alpha'} = g_s^{-1} \left(f_1^{-1} \left\{(W-2)dt^2 + W\, dz^2 - 2(W-1)\, dt\, dz\right\} + dx^i dx_i + f_5 \left(dr^2 + r^2\, g_{S^3}\right)\right) .$$

S-duality followed by T-duality: The T-dual of this S-dual configuration (5.21) along the circle parameterized by z explains the self-duality property discussed in the asymptotically AdS discussion in Sec. 5.3. Indeed, such a T-duality transformation interchanges the wave with the fundamental string, so that the resulting configuration has no modification in the geometry and fluxes. The configuration is given exactly by the set of equations (5.21) interchanging the role played by the harmonic functions f_1 and W, up to rescaling of coordinates.

T-duality: The T-dual description of the configuration (5.19)-(5.20) along the circle parameterized by z gives rise to a D0-D4 system with fundamental strings winding around the dual circle, in which all the D-branes are delocalized in the T-dual circle. The dilaton and fluxes describing this configuration are given by

$$\begin{aligned} e^{2\Phi} &= g_s^2\, W^{-1}\, f_1^{3/2}\, f_5^{-1/2}\ , \\ F_2 &= -g_s^{-1}\, df_1^{-1} \wedge dt\ , \\ F_4 &= 2Q_5\, \mathrm{dvol}\, S^3 \wedge dz\ , \\ H_3 &= dW^{-1} \wedge dt \wedge dz\ , \end{aligned} \tag{5.22}$$

whereas the metric is

$$\begin{aligned} \frac{g}{\alpha'} = f_1^{1/2}\, f_5^{-1/2}\, dx^i dx_i + (f_1 \cdot f_5)^{1/2}\, \left(dr^2 + r^2\, g_{S^3}\right) \\ - (f_1 \cdot f_5)^{-1/2}\, W^{-1}\, dt^2 + (f_1 \cdot f_5)^{1/2}\, W^{-1}\, dz^2\ . \end{aligned} \tag{5.23}$$

T-duality followed by M-theory lift: Finally, we could consider the strong coupling description of the T-dual configuration, where the eleventh dimension y opens up. This is expected to describe an M2-M5 system sharing one direction with momentum propagating along it. The eleven dimensional configuration is described by the metric

$$\begin{aligned} \frac{g}{l_p^2} = (g_s\, W)^{-2/3}\, f_5^{2/3}\, dy^2 + (g_s\, W)^{1/3}\, f_5^{-1/3}\, g_s^{-1}\, dx^i dx_i + (g_s\, W)^{1/3}\, f_5^{2/3}\, g_s^{-1}\, \left(dr^2 + r^2\, g_{S^3}\right) \\ + (g_s\, W)^{-2/3}\, f_5^{-1/3}\, \left\{(f_1 - 2)\, dt^2 + 2(f_1 - 1)\, dt dz + f_1\, g_s^2\, dz^2\right\}\ , \end{aligned} \tag{5.24}$$

and the four-form field strength

$$F_4 = dW^{-1} \wedge dt \wedge dz \wedge dy - 2Q_5 \mathrm{dvol}\, S^3 \wedge dy\ . \tag{5.25}$$

5.5 Towards a matrix model description

The string dualities described in Sec. 5.3 and the related asymptotically flat brane constructions in Sec. 5.4 relate our spacetime to matrix model descriptions. First, note again, as in Sec. 5.1 that our orbifold has a description in terms of a Penrose-like limit of the D1-D5 string wound on a circle with left-moving momentum, and, correspondingly, in terms of a DLCQ of the D1-D5 CFT. Let the charges of these branes and momenta be (Q_1, Q_5, n).

T-duality along the common circle direction produces a D0-D4-F1 system in IIA theory with charges (Q_1, Q_5, n), where now n measures the winding of the F1s along the T-dual circle. When

the charge Q_1 is very large the entire configuration should be describable in a $U(Q_1)$ matrix quantum mechanics associated with the D0s. Equivalently, the lift to M-theory of this configuration describes a M2-M5-p system with n M2s intersecting the $Q5$ M5s on the 11th circle with $Q1$ units of momentum. In the limit of large Q1, this background can be described as a state in the BFSS matrix model [40] which is again a matrix mechanics.

The S-dual of our orbifold in Secs. 5.3 and 5.4 arises as Penrose-like limit of of the F1-NS5 system in IIB string theory with momentum along the common direction and charges $(Q1, Q5, n)$. The Penrose-like limit corresponds to a low-energy limit in a sector where the momentum is going to infinity. This is precisely a scenario in which the $(0, 2)$ worldvolume theory on the NS5-branes reduces to a quantum mechanics since the 5-brane is wrapped on a 4-torus and a circle. What is more, the large momentum n implies a DLCQ of the $(0, 2)$ theory [41] and is thus related to quantum mechanics on the n instanton moduli space of a $U(Q_5)$ gauge theory in four dimensions. The fundamental strings will be represented as a certain state of this quantum mechanics. This again leads to a description in a matrix quantum mechanics. Interestingly, as we showed earlier, the F1-NS5-p system is self-dual under T-duality. This self-duality must manifest itself in the matrix model description. We can also exchange the M-theory circle with the circle in the IIA NS5-F1-p solution. This gives a M5-M2-p system in M-theory with n units of momentum along the common direction of the M5 and the M2. As described in Sec. 5.1 the Penrose-like limit leading to our orbifold geometry arises is a large n limit. Thus our background will arise as a state in the BFSS matrix model describing longitudinal M5 and M2 branes.

6. Conclusion

In this paper we have examined an interesting orbifold of AdS_3 by boosts and established many intriguing properties and connections with other corners of string theory. The boundary of our space contains two "null cylinders" and we established that a DLCQ of the D1-D5 string appears in the holographic description. We also showed that from several perspectives a matrix model is involved in holography, a fact which is particularly interesting because our orbifold is the universal geometry in the vicinity of the finite area extremal black holes of string theory in 4d and 5d and also of the BTZ black holes. As we discussed, it is natural to compactify our orbifold to two dimensions, and so we can also regard these comments as indicating a relation between certain 2d string theories and corresponding matrix models. This seems intriguing, although there is no direct connection between this observation and the $c = 1$ matrix model description of 2d bosonic string theory. Note also, that the various S and T dualities of our orbifold imply corresponding dualities between the various matrix model and DLCQ holographic descriptions of the spacetime.

A productive methodology in the study of pp-waves was to implemented the Penrose limit as an operation in the dual to the full AdS spacetime thereby isolating a sector of the full CFT that described just the pp-wave. A useful way of making progress here might be to consider an analogous operation focusing on a sector of the dual to the BTZ hole hole which has also been extensively studied. It would also be interesting to consider our orbifold as a solution in the Chern-Simons

description of 3d gravity and to explore excitations of this background such conical defects which arise from additional orbifolding. String theory on the orbifold can also be studied by explicitly constructing orbifolds of the WZW model description $\mathrm{AdS}_3 \times S^3$.

Our spacetime does not have a natural Euclidean continuation, hence its interest as a laboratory for the study of time dependent string theory. From many perspectives we saw that important properties of the spacetime and its dual are controlled by the structure of the complexified manifold constructed by continuing all the coordinates to complex values. For example, excursions in the complex coordinate plane transported real points in the spacetime to other real locations, and a singularity at an imaginary radial coordinate controlled the structure of normalizable wave solutions. This is reminiscent of the importance of the analytic structure and geodesics in the complex coordinate plane for recent investigations of "seeing holographically behind a horizon" [6]. A general lesson to be learned from all of these works might well be that even in the absence of a Euclidean continuation for a general time dependent universe, physical properties are nevertheless controlled by the analytic structure of complexified spacetime.

Acknowledgements

We are grateful to Micha Berkooz, Jan de Boer, Ben Craps, Jose Figueroa-O' Farrill, Eric Gimon, Esko Keski-Vakkuri, Matt Kleban, Per Kraus, Tommy Levi, Liat Maoz, Emil Martinec, Djordje Minic, Simon Ross, Kostas Skenderis, Andy Strominger and Jan Troost for interesting conversations at various stages in this project. Part of this work was completed at the Aspen Center for Physics. JS would like to thank the University of Chicago, the Institute for Advanced Studies in Princeton and the Perimeter Institute for kind hospitality during the different stages involved in this project. JS was supported by a Marie Curie Fellowship of the European Community programme "Improving the Human Research Potential and the Socio-Economic Knowledge Base" under the contract number HPMF-CT-2000-00480, during the initial stages of this project, by the Phil Zacharia fellowship from January to August in 2003. The travelling budget of JS was also supported in part by a grant from the United States–Israel Binational Science Foundation (BSF), the European RTN network HPRN-CT-2000-00122 and by Minerva, during the initial stages of this project. JS would also like to thank the IRF Centers of Excellence program. AN was supported in part by Stiching FOM. Work on this project at Penn was supported by the DOE under grant DE-FG02-95ER40893 and by the NSF under grant PHY-0331728.

A. Two point functions in momentum space

The Fourier transform of G_{++} is:

$$\tilde{G}_{++}(\omega, p) = \int_{-\infty}^{\infty} dt \int_{-\infty}^{\infty} d\phi \; e^{i\omega t} e^{ip\phi} G_{++}(t, \phi) = \frac{i}{2\pi R}\, h(\omega)\, g(p) \tag{A.1}$$

where h and g are the Fourier transforms of the t and ϕ dependent parts respectively. (Since G_{++} is periodic in ϕ the integral over the latter will yield a delta function that forces p to be an integer.)

We will do this transform by analytic continuation of the integral

$$\int_0^\infty e^{-\alpha x}\,(\sinh\beta z)^\gamma\,dx = \frac{1}{2^{\gamma+1}\beta}\,B(\alpha/2\beta-\gamma/2,\gamma+1) \tag{A.2}$$

where B is the beta function

$$B(x,y) = \frac{\Gamma(x)\Gamma(y)}{\Gamma(x+y)} \tag{A.3}$$

and the integral assumes $\mathrm{Re}(\beta)>0$, $\mathrm{Re}(\gamma)>-1$, $\mathrm{Re}(\alpha)>\mathrm{Re}(\beta\gamma)$.

Consider the integral over ϕ first. Let

$$g_n(p) = \int_{-\infty}^{\infty} d\phi\; e^{ip\phi}[\sinh(\phi+2\pi n)]^{-2h_+} \tag{A.4}$$

Since the range of ϕ is unbounded in the integral we can shift the integrand getting

$$g_n(p) = e^{-i2\pi pn}\int_{-\infty}^{\infty} d\phi\; e^{ip\phi}[\sinh(\phi)]^{-2h_+} = e^{-i2\pi pn}g_0(p) \tag{A.5}$$

Thus

$$g(p) = \sum_{n=-\infty}^{n=\infty} e^{-i2\pi pn}g_0(p) = g_0(p)\,\delta(p-m) \quad ; \quad m\in Z \tag{A.6}$$

To compute $g_0(p)$ we split the integral over positive and negative ϕ using $\sinh(-\phi)=-\sinh(\phi)$. This gives

$$g_0(p) = \int_{-\infty}^{\infty} d\phi\; e^{ip\phi}(\sinh\phi)^{-2h_+} \tag{A.7}$$

$$= \int_0^\infty d\phi\; e^{ip\phi}(\sinh\phi)^{-2h_+} + (-1)^{2h_+}\int_0^\infty d\phi\; e^{-ip\phi}(\sinh\phi)^{-2h_+} \tag{A.8}$$

We do these integrals by using (A.2) and analytically continuing the parameters in the equation above as

$$\gamma = -2h_+ + a \quad ; \quad \beta = 1 \quad ; \quad \alpha = -ip + b \tag{A.9}$$

with a and b large enough so that the conditions for the validity of (A.2) are satisfied. We then apply (A.2) and continue $a,b\to 0$. This gives

$$g_0(m) = \frac{\Gamma(1-2h_+)}{2^{1-2h_+}}\left[\frac{\Gamma(-im/2+h_+)}{\Gamma(-im/2+h_-)} + (-1)^{-2h_+}\frac{\Gamma(im/2+h_+)}{\Gamma(im/2+h_-)}\right] \tag{A.10}$$

Similarly, the Fourier transform of the time part of G_{++} gives

$$h(\omega) = \frac{\Gamma(1-2h_+)}{(2i)^{1-2h_+}}\left[\frac{\Gamma(-\omega/2+h_+)}{\Gamma(-\omega/2+h_-)} + (-1)^{-2h_+}\frac{\Gamma(\omega/2+h_+)}{\Gamma(\omega/2+h_-)}\right] \tag{A.11}$$

Multiplying everything together we find

$$\tilde{G}_{++}(\omega,m) = \frac{i}{2\pi R}\,(-1)^{-2h_+}\frac{1}{4}\left(\frac{i}{2}\right)^{2h_+-1}\frac{1}{2^{2h_+}}\,(\Gamma(1-2h_+))^2\,\frac{\Gamma(h_+-im/2)}{\Gamma(h_--im/2)}\,\frac{\Gamma(-\omega/2+h_+)}{\Gamma(-\omega/2+h_-)}$$
$$\times\left(e^{i\theta}+(-1)^{-2h_+}\right)\left\{\frac{\sin(\pi(\omega/2+h_-))}{\sin(\pi(\omega/2+h_+))}+(-1)^{-2h_+}\right\}\ . \tag{A.12}$$

where we used the relation

$$\Gamma(z)\Gamma(1-z) = \pi \csc \pi z \tag{A.13}$$

several times and the definition

$$\frac{\csc\Big(\pi(h_+ + \frac{im}{2})\Big)}{\csc\Big(\pi(h_- + \frac{im}{2})\Big)} = e^{i\theta}\,. \tag{A.14}$$

References

[1] H. Liu, G. Moore and N. Seiberg, *Strings in a time-dependent orbifold*, JHEP **0206**, 045 (2002) arXiv:hep-th/0204168;
J. Simón, *The geometry of null rotation identifications*, JHEP **0206**, 001 (2002) arXiv:hep-th/0203201;
L. Cornalba and M. S. Costa, *A new cosmological scenario in string theory*, Phys. Rev. D **66**, 066001 (2002) arXiv:hep-th/0203031;
V. Balasubramanian, S. F. Hassan, E. Keski-Vakkuri and A. Naqvi, *A space-time orbifold: A toy model for a cosmological singularity*, Phys. Rev. D **67**, 026003 (2003) arXiv:hep-th/0202187;
M. Fabinger and J. McGreevy, *On smooth time-dependent orbifolds and null singularities*, JHEP **0306**, 042 (2003) arXiv:hep-th/0206196;
G. T. Horowitz and J. Polchinski, *Instability of spacelike and null orbifold singularities*, Phys. Rev. D **66**, 103512 (2002) arXiv:hep-th/0206228;
L. Cornalba and M. S. Costa, *Time-dependent orbifolds and string cosmology*, Fortsch. Phys. **52**, 145 (2004) arXiv:hep-th/0310099.

[2] J. Khoury, B. A. Ovrut, P. J. Steinhardt and N. Turok, *The ekpyrotic universe: Colliding branes and the origin of the hot big bang*,Phys. Rev. D **64**, 123522 (2001) arXiv:hep-th/0103239;
M. Berkooz, B. Craps, D. Kutasov and G. Rajesh, *Comments on cosmological singularities in string theory*, JHEP **0303**, 031 (2003) arXiv:hep-th/0212215;
S. Elitzur, A. Giveon, D. Kutasov and E. Rabinovici, *From big bang to big crunch and beyond*, JHEP **0206**, 017 (2002) arXiv:hep-th/0204189;
B. Pioline and M. Berkooz, *Strings in an electric field, and the Milne universe*, JCAP **0311**, 007 (2003) arXiv:hep-th/0307280.

[3] G. T. Horowitz and D. Marolf, *A new approach to string cosmology*, JHEP **9807**, 014 (1998) arXiv:hep-th/9805207;
J. M. Maldacena, *Eternal black holes in Anti-de-Sitter*, JHEP **0304** (2003) 021. arXiv:hep-th/0106112.

[4] V. Balasubramanian, P. Kraus, A. E. Lawrence and S. Trivedi, *Holographic Probes of Anti-deSitter Spacetimes*, Phys. Rev. **D59**, (1999) 104021. arXiv:hep-th/9808117.

[5] S. Hemming, E. Keski-Vakkuri and P. Kraus, *Strings in the extended BTZ spacetime*, JHEP **0210**, 006 (2002) arXiv:hep-th/0208003.

[6] P. Kraus, H. Ooguri and S. Shenker, *Inside the horizon with AdS/CFT*, Phys. Rev. **D 67** (2003) 124022. arXiv:hep-th/0212277;
T. S. Levi and S. F. Ross, *Holography beyond the horizon and cosmic censorship*, Phys. Rev. **D 68** (2003) 044005. arXiv:hep-th/0304150;

L. Fidkowski, V. Hubeny, M. Kleban and S. Shenker, *The black hole singularity in AdS/CFT*. arXiv:hep-th/0306170.

[7] A. Strominger, *The dS/CFT Correspondence*, JHEP **0110** (2001) 034. arXiv:hep-th/0106113;
A. Strominger, *Inflation and the dS/CFT correspondence*, JHEP **0111**, 049 (2001) arXiv:hep-th/0110087;
V. Balasubramanian, J. de Boer and D. Minic, *Mass, Entropy and Holography in Asymptotically de Sitter Spaces*, Phys. Rev. **D65** (2002) 123508. arXiv:hep-th/0110108;
V. Balasubramanian, J. de Boer and D. Minic, *Exploring de Sitter Space and Holography*, Class. Quant. Grav. **19** (2002) 5655-5700. Annals Phys. **303** (2003) 59-116. arXiv:hep-th/0207245.

[8] M. I. Park, *Statistical entropy of three-dimensional Kerr-de Sitter space*, Phys. Lett. B **440**, 275 (1998) arXiv:hep-th/9806119;
M. I. Park, *Symmetry algebras in Chern-Simons theories with boundary: Canonical approach*, Nucl. Phys. B **544**, 377 (1999) arXiv:hep-th/9811033.

[9] M. Banados, C. Teitelboim and J. Zanelli, *The Black Hole In Three-Dimensional Space-Time*, Phys. Rev. Lett. **69**, 1849 (1992) arXiv:hep-th/9204099;
M. Banados, M. Henneaux, C. Teitelboim and J. Zanelli, *Geometry of the 2+1 black hole*, Phys. Rev. **D 48** (1993) 1506-1525 . arXiv:gr-qc/9302012.

[10] G. J. Galloway, K. Schleich, D. Witt and E. Woolgar, *The AdS/CFT correspondence conjecture and topological censorship*, Phys. Lett. B **505**, 255 (2001) arXiv:hep-th/9912119.

[11] O.Coussaert and M. Henneaux, *Self-dual solutions of 2+1 Einstein gravity with negative cosmological constant*, arXiv:hep-th/9407181.

[12] D. A. Lowe and A. Strominger, *Exact four-dimensional dyonic black holes and Bertotti-Robinson space-times in string theory*, Phys. Rev. Lett. **73**, 1468 (1994). arXiv:hep-th/9403186.

[13] A. Strominger, AdS_2 *Quantum gravity and String Theory*, JHEP **9901** (1999) 007. arXiv:hep-th/9809027.

[14] J. M. Maldacena, J. Michelson and A. Strominger, *Anti-de Sitter Fragmentation*, JHEP **9902** (1999) 011. arXiv:hep-th/9812073;
M. Spradlin and A. Strominger, *Vacuum States for* AdS_2 *Black Holes*, JHEP **9911** (1999) 021. arXiv:hep-th/9904143.

[15] V. Balasubramanian, P. Kraus and A. E. Lawrence, *Bulk vs. boundary dynamics in anti-de Sitter spacetime*, Phys. Rev. **D59**, (1999) 046003. arXiv:hep-th/9805171.

[16] E. Witten, *Anti-de Sitter space and holography*, Adv. Theor. Math. Phys. **2** (1998) 253. arXiv:hep-th/9802150;
S. S. Gubser, I. R. Klebanov and A. M. Polyakov, *Gauge theory correlators from non-critical string theory*, Phys. Lett. **B428** (1998) 105 arXiv:hep-th/9802109.

[17] J. M. Figueroa-O'Farrill and J. Simón, *Supersymmetric Kaluza–Klein reductions of AdS backgrounds* arXiv:hep-th/0401206.

[18] O. Madden and S. F. Ross, *Quotients of anti-de Sitter space* arXiv:hep-th/0401205.

[19] Y. Kosmann, *Dérivées de Lie des spineurs*, Annali di Mat. Pura Appl. (IV) **91** (1972), 317–395.

[20] JM. Figueroa-O'Farrill, *On the supersymmetries of Anti-de Sitter vacua*, Class. Quant. Grav. **16** (1999), 2043–2055, arXiv:hep-th/9902066.

[21] C .P. Burgess and C. A. Lütken, *Propagators and effective potentials in anti-de Sitter space*, Phys. Lett. **B153** (1985) 137-141.

[22] J. M. Maldacena, *The large N limit of superconformal field theories and supergravity*, Adv. Theor. Math. Phys. **2** (1998) 231. [Int. J. Theor. Phys. **38**, 1113 (1999)] arXiv:hep-th/9711200.

[23] D. Z. Freedman, S. D. Mathur, A. Matusis and L. Rastelli, *Correlation functions in the CFT(d)/AdS(d + 1) correspondence*, Nucl. Phys. **B546** (1999) 96. arXiv:hep-th/9804058.

[24] E. Keski-Vakkuri, *Bulk and boundary dynamics in BTZ black holes*, Phys. Rev. D **59** (1999), 104001, arXiv:hep-th/9808037.

[25] V. Balasubramanian, S. B. Giddings and A. E. Lawrence, *What do CFTs tell us about anti-de Sitter spacetimes?*, JHEP **9903** (1999) 001 (1999). arXiv:hep-th/9902052;
S. B. Giddings, *The boundary S-matrix and the AdS to CFT dictionary*, Phys. Rev. Lett. **83** (1999) 2707. arXiv:hep-th/9903048;
T. Banks, M. R. Douglas, G. T. Horowitz and E. J. Martinec, *AdS dynamics from conformal field theory.* arXiv:hep-th/9808016.

[26] P. Ginsparg and G. W. Moore, *Lectures On 2-D Gravity And 2-D String Theory.* arXiv:hep-th/9304011.

[27] A. Strominger,*Black hole entropy from near-horizon microstates,*. JHEP **9802** (1998) 009. arXiv:hep-th/9712251.

[28] A. Strominger and C. Vafa, *Microscopic Origin of the Bekenstein-Hawking Entropy*, Phys. Lett. **B379** (1996) 99. arXiv:hep-th/9601029.

[29] J. M. Maldacena and A. Strominger, *Statistical Entropy of Four-Dimensional Extremal Black Holes*, Phys. Rev. Lett. **77** (1996) 428. arXiv:hep-th/9603060;
C. V. Johnson, R. R. Khuri and R. C. Myers, *Entropy of 4D Extremal Black Holes*, Phys. Lett. B **378** (1996) 78. arXiv:hep-th/9603061;
V. Balasubramanian and F. Larsen, *On D-Branes and Black Holes in Four Dimensions*, Nucl. Phys. **B478** (1996) 199-208. arXiv:hep-th/9604189.

[30] V. Balasubramanian and F. Larsen, *Near horizon geometry and black holes in four dimensions*, Nucl. Phys. **B528** (1998) 229-237 arXiv:hep-th/9802198.

[31] M. Cvetic, H. Lu, C. N. Pope, *Spacetimes of boosted p-branes, and CFT in Infinite-momentum frame*, Nucl. Phys. **B545** (1999) 309-339 arXiv:hep-th/9810123.

[32] R. Penrose, *Any space-time has a plane wave as a limit*, in *Differential Geometry and relativity*, Cahen and Flato, eds., pp. 271-275. Reidel, Dordrecht-Holland, 1976.

[33] M. Blau, J. Figueroa-O'Farrill, C. Hull and G. Papadopoulos, *Penrose limits and maximal supersymmetry*, Class. Quant. Grav. **19**, L87 (2002) arXiv:hep-th/0201081;
M. Blau, J. Figueroa-O'Farrill and G. Papadopoulos, *Penrose limits, supergravity and brane dynamics*,Class. Quant. Grav. **19**, 4753 (2002) arXiv:hep-th/0202111.

[34] D. Marolf and S. F. Ross, *Plane waves and spacelike infinity*, Class. Quant. Grav. **20**, 4119 (2003) arXiv:hep-th/0303044;
D. Berenstein and H. Nastase, *On lightcone string field theory from super Yang-Mills and holography*, arXiv:hep-th/0205048.

[35] D. Berenstein, J. M. Maldacena and H. Nastase, *Strings in flat space and pp waves from N = 4 super Yang Mills*, JHEP **0204**, 013 (2002) arXiv:hep-th/0202021.

[36] R. Gueven, *Plane wave limits and T-duality*, Phys. Lett. **B 482**, 255 (2000) arXiv:hep-th/0005061;
N. Itzhaki, I. R. Klebanov and S. Mukhi, *PP wave limit and enhanced supersymmetry in gauge theories*, JHEP **0203**, 048 (2002) arXiv:hep-th/0202153;
J. Gomis and H. Ooguri, *Penrose limit of N = 1 gauge theories*, Nucl. Phys. **B 635**, 106 (2002) arXiv:hep-th/0202157;
M. Cvetic, H. Lu and C. N. Pope, *M-theory pp-waves, Penrose limits and supernumerary supersymmetries*,Nucl. Phys. **B 644**, 65 (2002). arXiv:hep-th/0203229.

[37] N. A. Obers and B. Pioline, *U-duality and M-theory*, Phys. Rept. **318** (1999) 113-225. arXiv:hep-th/9809039.

[38] J. M. Maldacena and A. Strominger, AdS_3 *Black Holes and a Stringy Exclusion Principle*, JHEP **9812** (1998) 005. arXiv:hep-th/9804085.

[39] T. Buscher, Phys. Lett. **B159** (1985) 127; *ibid* **B194** (1987) 59; *ibid* **B201** (1988) 466;
E. Bergshoeff, C. Hull and T. Ortín, *Duality in the type IIB superstring effective action*, Nucl. Phys. **B451** (1995) 547-578, arXiv:hep-th/9504081.

[40] T. Banks, W. Fischler, S. H. Shenker and L. Susskind, *M theory as a matrix model: A conjecture*, Phys. Rev. **D 55** (1997) 5112. arXiv:hep-th/9610043.

[41] O. Aharony, M. Berkooz, S. Kachru, N. Seiberg and E. Silverstein, *Matrix description of interacting theories in six dimensions*, Adv. Theor. Math. Phys. **1** (1998) 148. arXiv:hep-th/9707079;
O. Aharony, M. Berkooz and N. Seiberg, *Light-cone description of (2,0) superconformal theories in six dimensions*, Adv. Theor. Math. Phys. **2** (1998) 119. arXiv:hep-th/9712117;
O. Aharony, M. Berkooz, D. Kutasov and N. Seiberg, *Linear dilatons, NS5-branes and holography*, JHEP **9810** (1998) 004. arXiv:hep-th/9808149;
O. Aharony and M. Berkooz, *IR dynamics of d = 2, N = (4,4) gauge theories and DLCQ of 'little string theories'*, JHEP **9910** (1999) 030. arXiv:hep-th/9909101.

[42] D. T. Son and A. O. Starinets, *Minkowski-space correlators in AdS/CFT correspondence: Recipe and applications*, JHEP **0209**, 042 (2002). arXiv:hep-th/0205051;
Y. Satoh and J. Troost, *On time-dependent AdS/CFT*, JHEP **0301**, 027 (2003). arXiv:hep-th/0212089;
V. Balasubramanian, T. S. Levi and A. Naqvi, *A comment on multiple vacua, particle production and the time dependent AdS/CFT correspondence*, arXiv:hep-th/0303157.